DESIGN PARAMETERS FOR SOLAR POWERED ABSORPTION

COOLING SYSTEMS WITH CHILLED WATER STORAGE

By

PING-SHIAN SHIH

Bachelor of Science in Engineering
National Taiwan University
Taipei, Taiwan
1971

Master of Science in Mechanical Engineering
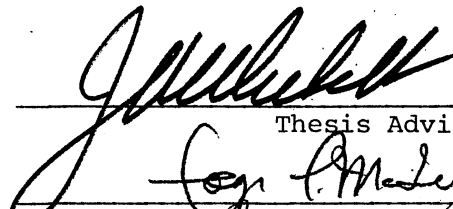University of New Hampshire
Durham, New Hampshire
1976

Submitted to the Faculty of the Graduate College
of the Oklahoma State University
in partial fulfillment of the requirements
for the Degree of
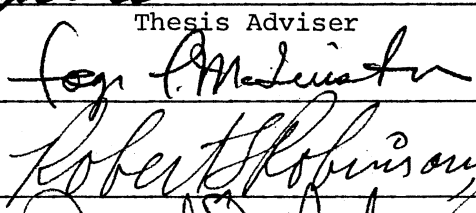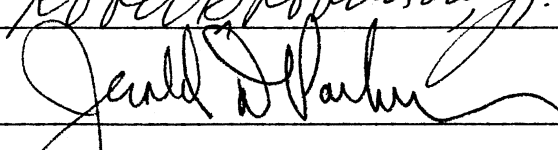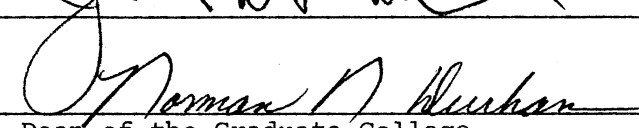DOCTOR OF PHILOSOPHY
December, 1979

DESIGN PARAMETERS FOR SOLAR POWERED ABSORPTION

COOLING SYSTEMS WITH CHILLED WATER STORAGE

Thesis Approved:

_____
Thesis Adviser

_____

_____

_____

_____
Dean of the Graduate College

ACKNOWLEDGMENTS

I would like to express my sincere appreciation to my adviser, Dr. John A. Wiebelt, for his continued interest and patient guidance throughout this study, and for his help in the preparation of this thesis.

Special thanks are extended to Dr. Faye C. McQuiston and Dr. Jerald D. Parker for their helpful comments and suggestions. Thanks are also due to Dr. Robert L. Robinson, Jr. for serving on the advisory committee.

I am grateful to Dr. John P. Chandler for letting me use his excellent nonlinear least squares analysis program, MARQ.

The School of Mechanical and Aerospace Engineering and the School of Technology of the Oklahoma State Univeristy are acknowledged for providing me with financial assistance during the course of this study.

I would like to thank all my colleagues for their friendship and their contributions of time and advice.

Ms. Charlene Fries is acknowledged for her excellent work in typing the first and final manuscript.

I am grateful to my brothers, Ping-Chien, Ping-Wen, Ping-Yho, Ping-Fhun, and to my sisters, Sheue-Fuea, Jui-Fuea, Kuei-Fuea, for their constant financial and spiritual support throughout my undergraduate and graduate years. And above all, I wish to express a special gratitude to my mother, Mrs. Show-Ching Shih, for her love and sacrifice. To my mother and to the memory of my late father, Dr. Ting-Liao Shih, I dedicate this thesis.

TABLE OF CONTENTS

TABLE

LIST OF FIGURES

NOMENCLATURE

A_c — solar energy collector area

C — capacitance rate, $\dot{m}C_p$

C_A — cost of solar energy collector and its associate components per unit collector area; cost of the first category solar cooling system components

C_E — total cost of solar cooling system components that are not related to either the solar energy collector or the storage tank; cost of the third category solar cooling system components

C_F — fuel cost; energy cost

C_p — specific heat

C_S — cost of storage tank and its associate components per unit storage tank volume; cost of the second category solar cooling system components

e — real growth rate of the fuel cost

F' — solar energy collector efficiency factor

F_R — solar energy collector heat removal factor

g_o, g_1, g_2 — room air transfer function coefficients

H_T — solar radiation incident per unit area on a tilt surface

i — interest rate; discount rate

L — seasonal total cooling load

M — total mass of the storage water

$\dot{m}$ — mass flow rate

N — number of days in the cooling season

n — component lifetimes

P — initial investment

p_o, p_1	room air transfer function coefficients
$\dot{Q}$	heat transfer rate
$\dot{Q}_c$	absorption chiller capacity
$\dot{Q}_{HE}$	heat transfer rate of a heat exchanger
$\dot{Q}_h$	energy input per hour to the absorption chiller
$\dot{Q}_u$	useful energy gain of a solar energy collector
$\dot{Q}_x$	heat extraction rate
R	annual cost of ownership
S	seasonal total solar radiation incident per unit collector area
SEER	seasonal energy efficiency ratio of a reciprocating chiller
SF	solar fraction
T	temperature
T_a	ambient dry bulb temperature
$\bar{T}_{DB}$	design dry bulb temperature
T_h	heat source temperature; collector fluid temperature; hot storage water temperature
T_i	collector fluid inlet temperature
T_ℓ	refrigeration load temperature; chilled water temperature
T_r	room air temperature
T_{rc}	constant room temperature used for calculating cooling load
T_s	heat sink temperature; condensing water temperature
T_{WB}	ambient wet bulb temperature
U_L	solar energy collector overall energy loss coefficient
V_c	chilled water storage tank volume
V_H	hot water storage tank volume

α	collector cover plate absorptance for light
ε	heat exchanger effectiveness
ρ	density
τ	collector cover plate transmittance for light

Subscripts

i; in	refer to property at the inlet
m	at year m
o; out	refer to property at the outlet
0	at year zero
Δ	one increment of time

Superscript

*	indicates nondimensionalized parameter

CHAPTER I

INTRODUCTION

Using solar energy to power an absorption chiller for space cooling is highly desirable because it conserves nonrenewable conventional energy sources and because combining solar cooling with a solar heating system can make the overall system more cost effective. However, there are several problems which must be solved before solar cooling can be employed extensively. The most important problems are the low efficiency of the solar energy collector and the low COP of the absorption chiller when fired with 75 to 95°C water, and the severe degrading of the COP of the absorption chiller in the real working environment. Recent developments of solar energy collectors and absorption chillers have improved considerably the efficiency of the collectors and the COP of the chillers. However, the degrading of the COP of the absorption chiller remains to be addressed.

The degrading of the COP of the absorption chiller is largely due to the frequent on-off cycling of the chiller during medium and low cooling demand periods and the unfavorable working conditions caused by the time difference between the peak cooling demand and the peak solar radiation. The present study is an evaluation of the feasibility of using chilled water storage as a buffer to reduce the effects of these two undesirable working conditions and to improve the performance of the absorption chiller as well as the entire solar cooling system.

In solar cooling systems with no chilled water storage, the absorption chiller is connected directly to the air handling unit. In these systems, the absorption chiller is controlled by the cooling demand and the heat source temperature which is the hot water storage tank temperature. Because large variations exist in the cooling demand distribution each day and also from day to day, the absorption chiller designed to satisfy the peak cooling demand will be operated on and off with very short operating periods during medium and low cooling demands. In addition to this, the hot water storage tank temperature has its own temperature distribution cycles corresponding to the solar radiation distribution which generally peaks four to six hours earlier than the cooling demand. Therefore, the absorption chiller operates under unfavorable working conditions most of tne time which results in the degradation of the COP. If one employs a chilled water storage tank between the absorption chiller and the air handling unit, the constraint on the chiller due to the variation of the cooling demand is released. The absorption chiller in this case is not required to produce cooling as demanded by the conditioned space; instead it is controlled by the temperature of the chilled water storage tank and hot water storage tank. The sizes of the chilled water storage, the hot water storage, and the collector area can then be designed according to the general patterns of the weather and cooling demend to provide the best possible working conditions for the absorption chiller.

The present study has the following three principal objectives:

1. To confirm the feasibility of using chilled water storage to reduce the degradation of the COP of the absorption chiller and to investigate the relationship between the sizes of the chilled water storage,

the hot water storage, the collector area, and the performance of the absorption chiller as well as the entire cooling system.

2. To develop a semi-empirical equation for predicting the performance of the solar cooling system with chilled water storage.

3. To develop a general procedure of evaluating and optimizing the economics of the solar cooling system.

CHAPTER II

LITERATURE SURVEY

The idea of utilizing solar energy to operate absorption chillers
for space cooling has been attracting researchers for more than two de-
cades. In 1958, Eisenstadt et al. (1) showed that absorption chillers
using high concentration ammonia-water solution as a working fluid could
be operated with low temperatures that are obtainable by flat plate col-
lectors. In 1962, Chung et al. (2) also demonstrated that lithium
bromide-water absorption chillers could be operated with solar energy.
In succeeding years, there were several other literature citations re-
porting the use of solar energy powered absorption chillers for space
cooling (3) (4) (5).

In these early studies of solar energy powered absorption chillers,
several problems were identified. The most important problems are the
low COP of the absorption chiller and the low efficiency of the solar
energy collector operating in the required temperature range of 75 to
95°C. Subsequent research efforts more or less concentrated on improv-
ing these two deficiencies.

Research efforts on solar energy collectors were relatively more in-
tensive and successful, especially so in the case of the flat plate col-
lector. The main problem of the flat plate collector is its low effi-
ciency operating at the high temperature range required by the absorption
chiller. This low efficiency is the result of an increase of heat loss

4

to the environment. Many schemes to reduce this heat loss have been proposed. Charters and Peterson (6), Pellette, Cobble, and Smith (7) examined the use of honeycomb to reduce the convection heat loss. Eaton and Blum (8) proposed using a moderate vacuum in the space between the cover plate and absorber plate. Minardi and Chuang (9) studied the use of a black liquid to improve the collector efficiency. Perhaps the most successful scheme was to apply a selective surface coating on the absorber plate ((10) through (17)). One other scheme that is very helpful is to use low-iron and anti-reflection coated glass for cover plates (18). The efficiency of the collector treated with these two methods can be in the range of 0.4 to 0.6 operating in the temperature range between 75°C and 95°C.

Compared with the development of the falt plate solar energy collector, the development of the absorption chiller for solar cooling systems was not as successful. The low COP of the absorption chiller is due to a low temperature heat source (19) (20) (21). In an effort to improve the COP, several absorbent-refrigerant pairs other than lithium bromide-water and ammonia-water have been studied. Sargent and Beckman (22) proposed to use ammonia-sodium thiocyanate to replace ammonia-water. Swartmen, Ha, and Swaminathan (23) compared the performance of these two absorption chillers. The ammonia-sodium thiocyanate pair eliminates the requirement of a rectifying column but does not lower the required heat source temperature. Farber, Morrison, and Ingley (24) compared several absorbent-refrigerant pairs and selected ammonia-water for their air-cooled absorption chiller. Ellington (25) and Macriss (26) conducted more comprehensive studies and concluded that lithium bromide-water absorption chiller yields the best COP. The only drawback of the lithium

bromide-water absorption chiller is its requirement of water cooling. Macriss (26) suggested adding another salt, such as lithium thiocyanate, to extend the crystallization temperature region and make air cooling possible. However, it also raises the required heat source temperature to above 120°C, which is out of the operating temperature range of most flat plate collectors. Some modified absorption refrigeration cycles such as multistage cycles have also been studied but without much success (27) (28). Between lithium bromide-water and ammonia-water absorption chillers, the former is favored for solar cooling applications because of its higher COP and lower temperature requirement (29) (30) (31). The lithium bromide-water absorption chiller specifically designed for solar energy applications can be operated with COP between 0.5 and 0.8 at a heat source temperature between 75 and 95°C (32). This performance is not ideal but is considered to be practical and acceptable.

An improved solar collector and lithium bromide absorption chiller were installed and evaluated in the Colorado State University Solar House I (33). The COP of the absorption chiller was measured to be about 0.6 during periods of high cooling demand, i.e., when cooling demand is near the designed value. But the COP dropped to nearly 0.3 during periods of medium and low cooling demand. Another experimental solar house in Japan also reported the same result (34). The degrading of the COP of the absorption chiller during medium and low cooling demand periods presented a new and serious problem, especially so when one considers the fact that most of the time the cooling demand is well below the design value.

Beckman (35) suggested that the degrading of the COP of the absorption chiller is partially due to start-up transients. Rauch and Wood

(36) studied the start-up transient performance of the ARKLA three-ton solar absorption chiller. They reported that the absorption chiller needs about ten minutes to start producing cooling and that the instantaneous COP reaches the steady state value only after about 20 minutes of operation. Thus the cumulative average COP is reduced to about half of the steady state average value when it is only operated for 30 minutes, 80 percent when operated for one hour, and 90 percent after two hours. To achieve a cumulative average COP that is comparable with steady state average performance, the chiller needs to be operated continuously for about three and one-half hours. The absorption chiller in the CSU solar house I recorded as many as 40 start-ups in one 24-hour period during low cooling demand. Therefore, the absorption chiller was operated for less than 30 minutes in each operation; as a result, the COP was reduced to about 0.3 (33).

One other reason for the low COP of absorption chillers is the transient characteristics of the heat source temperature, the cooling water temperature, and the cooling demand, as pointed out by Miller (37) and Newton (38). Generally speaking, the insolation reaches its maximum at solar noon and hence the heat source temperature. However, the cooling demand does not reach its maximum until four to six hours later. This time difference between the maximums of the heat source temperature and cooling demand causes the absorption chiller to operate at unfavorable conditions most of the time and produce cooling with low COP.

Beckman (35) reviewed some possible solutions for the degrading of the absorption chiller's performance. One is to deliberately underdesign the capacity of the chiller to force it to work more continuously. However, this scheme will lead to unsatisfactory performance during high

cooling demand periods because of the lack of capacity. The other

scheme is to use chilled water storage. Ward, Löf and Uesaki (39) de-

signed a system with chilled water storage for the Colorado State Uni-

versity Solar House III. However, their method for choosing the size of

the chilled water storage is based on the time desired for the chiller,

operating at its maximum capacity, to complete chilling the storage water

in the tank. This method only provides a coarse estimate of the required

size of the chilled water storage and the performance of the chiller.

The literature search indicated that there exists a new and serious

problem of solar cooling systems in the degrading of the absorption

chiller during medium and low cooling demand periods. The chilled water

storage offers an attractive solution to this problem, yet no systematic

investigation of this scheme has been reported in the literature. It is

therefore worthwhile to conduct a comprehensive study on this scheme.

CHAPTER III

THE ENERGY FACTOR OF THE SOLAR

ENERGY COOLING SYSTEM

The energy factor of the solar energy cooling system will be defined as the ratio of the heat removed from the conditioned space to the total solar radiation falling upon the collector surface. Because the solar energy collected is not necessarily processed immediately to produce cooling, the energy factor in this context is a time averaged factor and not an instantaneous one. Solar energy cooling systems are composed of many components, such as the solar energy collector, circulation pipes and pumps, energy storage tanks, absorption chiller, cooling tower, room air handling unit, etc. The energy factor of the system is a function of the efficiencies of all these components. The most important among these are the efficiency of the solar energy collector and the COP of the absorption chiller. The energy factor of the system is directly proportional to the product of these two terms. In this chapter these two major factors, namely the efficiency of the flat plate solar energy collector and the COP of the absorption chiller, will be examined. The role of the chilled water storage in improving the performance of these two components will also be discussed.

Efficiency of the Flat Plate Solar Energy Collector

The performance of a flat plate solar energy collector can usually

be described as an energy balance equation. The most celebrated of this type is the Hottel and Whillier (40) collector equation. It expresses the rate of total useful energy gain $\dot{Q}_u$ as

$$\dot{Q}_u = F_R A_c \left[H_T (\tau\alpha) - U_L (T_i - T_a) \right] \tag{3.1}$$

where

$$F_R = \frac{\dot{m} C_p}{U_L A_C} \left[1 - \exp \left(\frac{-F' U_L A_C}{\dot{m} C_p} \right) \right] \tag{3.2}$$

In this equation the collector heat removal factor F_R, the collector efficiency factor F', the collector overall energy loss coefficient U_L, and the transmittance-absorptance product, $\tau\alpha$, are related to the physical structure of the collector. Generally, these four parameters can be considered as constants for a given design and mass flow rate of collector fluid, and the equation still can predict the performance of the collector with reasonable accuracy (41). Therefore, the performance of a given collector is a function of only four parameters, namely the rate of total radiation incident on the collector surface H_T, the ambient temperature T_a, the fluid flow rate, and the fluid inlet temperature T_i. As can readily be seen in Equation (3.1), the performance of the collector is better when H_T and T_a are high and T_i is low. Since T_i is largely determined by the hot water storage tank temperature, it can be concluded that the lower the hot water storage tank temperature, the higher the collector efficiency.

COP of the Absorption Refrigeration Cycle

The basic absorption refrigeration cycle is comparable in some ways to a combination of a heat-engine and a vapor-compression refrigeration

cycle (42). Figure 1 illustrates the similarity of these two systems.
The COP of an ideal absorption refrigeration cycle is often written as

$$COP = (\frac{T_h - T_s}{T_h}) (\frac{T_\ell}{T_s - T_\ell})$$

where

T_h = absolute temperature of the heat source;

T_s = absolute temperature of the heat sink; and

T_ℓ = absolute temperature of the refrigeration load.

The first term on the right corresponds to the efficiency of a Carnot
cycle, whereas the second term is the COP of a reversed Carnot cycle
which is an ideal vapor-compression refrigeration cycle. It is obvious
that if one raised the heat source temperature and kept the other two
temperatures constant, the efficiency of the Carnot cycle will increase
while the COP of the reverse Carnot cycle remains constant. The result
is a higher COP of the system. On the other hand, raising the heat sink
temperature will lower the COP of the system. Based on this, one might
conclude that high heat source temperature and low heat sink temperature
is always desirable for the absorption refrigeration cycle. However,
for a real refrigeration cycle, higher heat source temperature does not
always result in higher COP.

The main reason for the departure of the real refrigeration cycle
from the ideal cycle lies in the fact that the refrigerant is super-
heated when it is separated from the absorbent in the generator. In
Figure 2 the absorbent and refrigerant cycles are plotted separately.
Since the refrigerant after evaporating in the evaporator, state 8, is
absorbed by the absorbent and will not be separated from the absorbent
until it reaches the generator, state 5, the process between these two
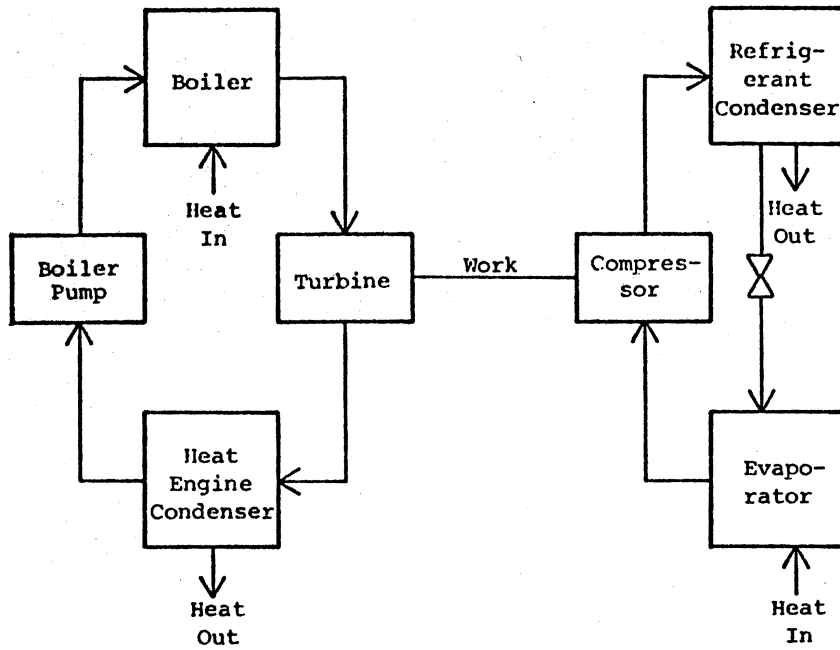
(a) Combination of Heat Engine Cycle and Vapor-
Compression Refrigeration Cycle
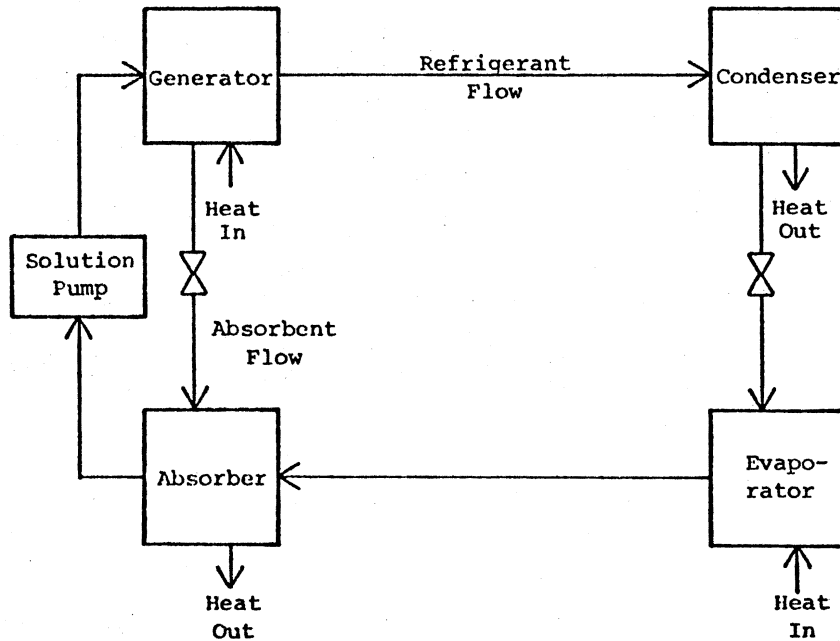
(b) Basic Absorption Refrigeration Cycle

Figure 1. Schematic of the Basic Absorption
Refrigeration Cycle and the Com-
bination of the Heat Engine and
Vapor Compression Refrigeration
Cycles
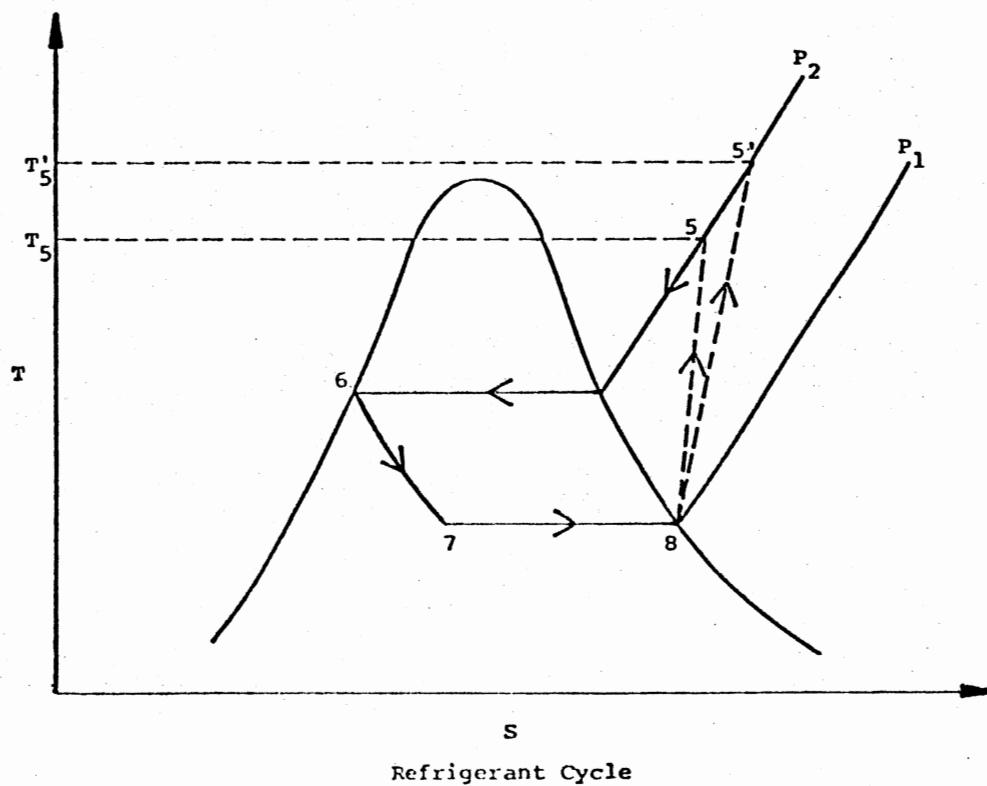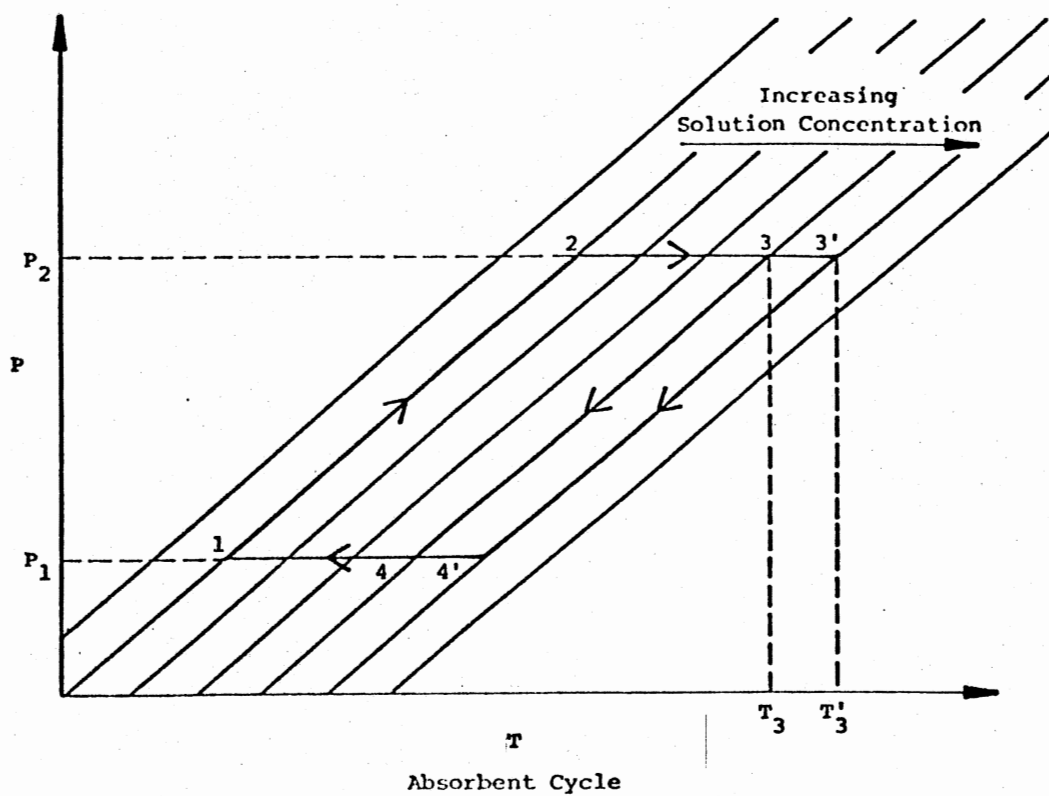
Figure 2. The Absorbent and Refrigerant Cycles

states cannot be represented in the T-S diagram of the refrigerant and therefore is only connected by a dashed line. The temperature of the strong absorbent and the refrigerant leaving the generator, T_3 and T_5, respectively, are equal to each other because both are in contact with the same heat source temperature. Furthermore, state 5 is always in the superheated region due to the fact that the addition of the absorbent raises the boiling temperature of the refrigerant. It can be proved that higher generator temperature, for example, T_3' instead of T_3, will improve the efficiency of the absorbent cycle. However, for the refrigerant cycle, being a reverse cycle, the same higher generator temperature, T_5', will result in lower COP. The effect on the COP of the system is determined by the balance of the gain of the absorbent cycle and the loss of the refrigerant cycle. When the generator temperature is relatively low, the gain is generally greater than the loss. Continuing increase of the generator temperature, however, will produce a lesser gain of the absorbent cycle due to the increase of the absorbent concentration. It will reach a point where the loss of the refrigerant cycle begins to outweigh the gain of the absorbent cycle. Further increase of the generator temperature will only lower the COP of the system. Figure 3 shows the COP and capacity data for a 25-ton absorption chiller (32). The COP clearly has a maximum around 82°C hot water inlet temperature. Note that the capacity at this point is only about 80 percent of the designed capacity.

Role of the Chilled Water Storage

The chilled water storage, apart from storing solar energy in the form of chilled water, has the following two important functions
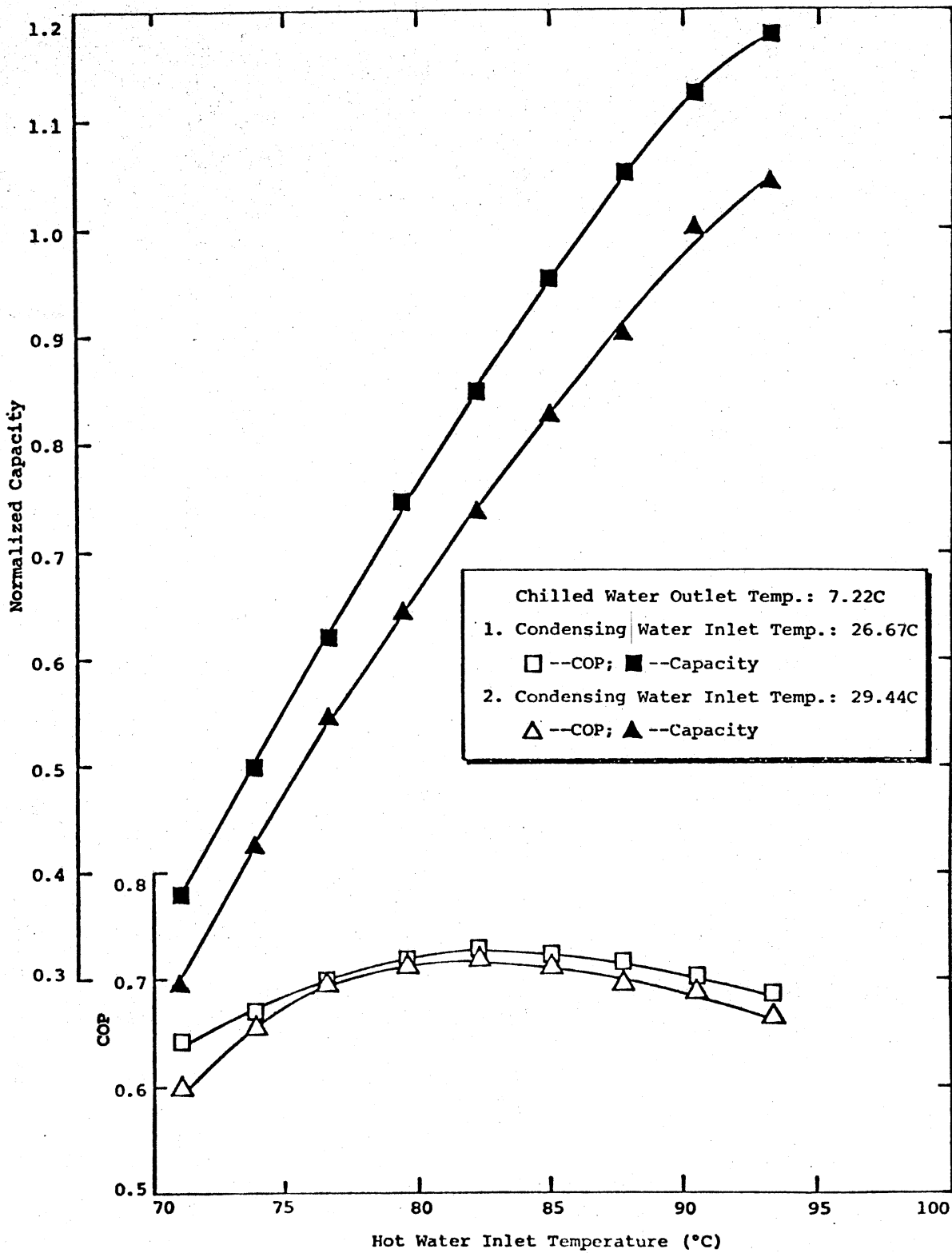
Figure 3. COP and Capacity Data for the ARKLA 25 Ton
           Absorption Chiller--Solaire 300 (Capaci-
           ties Were Normalized With Design Capa-
           city)

concerning the energy efficiency of the solar cooling system. First, it enables the absorption chiller to work more continuously. The absorption chiller is controlled by the temperature of the chilled water storage tank and the hot water storage tank. It is activated when the chilled water temperature is above the upper set temperature and continues working until the chilled water temperature is below the lower set temperature or the hot water tank temperature is below the minimum required heat source temperature of the chiller. In this manner the operation time of the chiller depends mainly on the sizes of the chilled water and hot water tanks and not on the uncontrollable cooling demand, as in the case of a system without chilled water storage.

Second, it enables the absorption chiller to work with higher COP. The absorption chiller performs with higher COP at a capacity about 80 percent of the designed capacity as mentioned in the previous section. In a system without chilled water storage, the chiller has to work at its designed capacity in order to meet the cooling demand during the high cooling demand period. Thus the chiller requires a higher heat source temperature and yet produces cooling with lower COP. With chilled water storage, the chiller can work with higher COP and lower heat source temperature, which in turn improves the collector efficiency.

CHAPTER IV

PERFORMANCE OF SOLAR ENERGY COOLING SYSTEMS

WITH CHILLED WATER STORAGE

The performance of a solar energy cooling system can generally be evaluated by detailed system simulations. Simulation methods are particularly useful for investigating the dynamic relationships between system components which if done by experiments will be too costly and time consuming. In this chapter the design of a solar cooling system and the formulation of its simulation model will be described. Simulations were done to study the performance of the system with respect to the sizes of the chilled water storage, hot water storage, and collector area.

The System Configuration

A schematic diagram of the solar cooling system is shown in Figure 4. The system uses double glazed, selective surface solar energy collector. An antifreeze solution is used as collector fluid to avoid the problems of freezing, boiling, and corrosion. The solar energy collected by the collector is transferred to the hot water storage tank through a heat exchanger, HE-1 in the diagram. A second heat exchanger, HE-2, is used to dissipate the heat when the hot water temperature becomes too high, for example, 95°C or above. The circulation of the collector fluid and hot water is controlled by a controller, C-1, which senses the temperature of the collector and the hot water. When the outlet

17
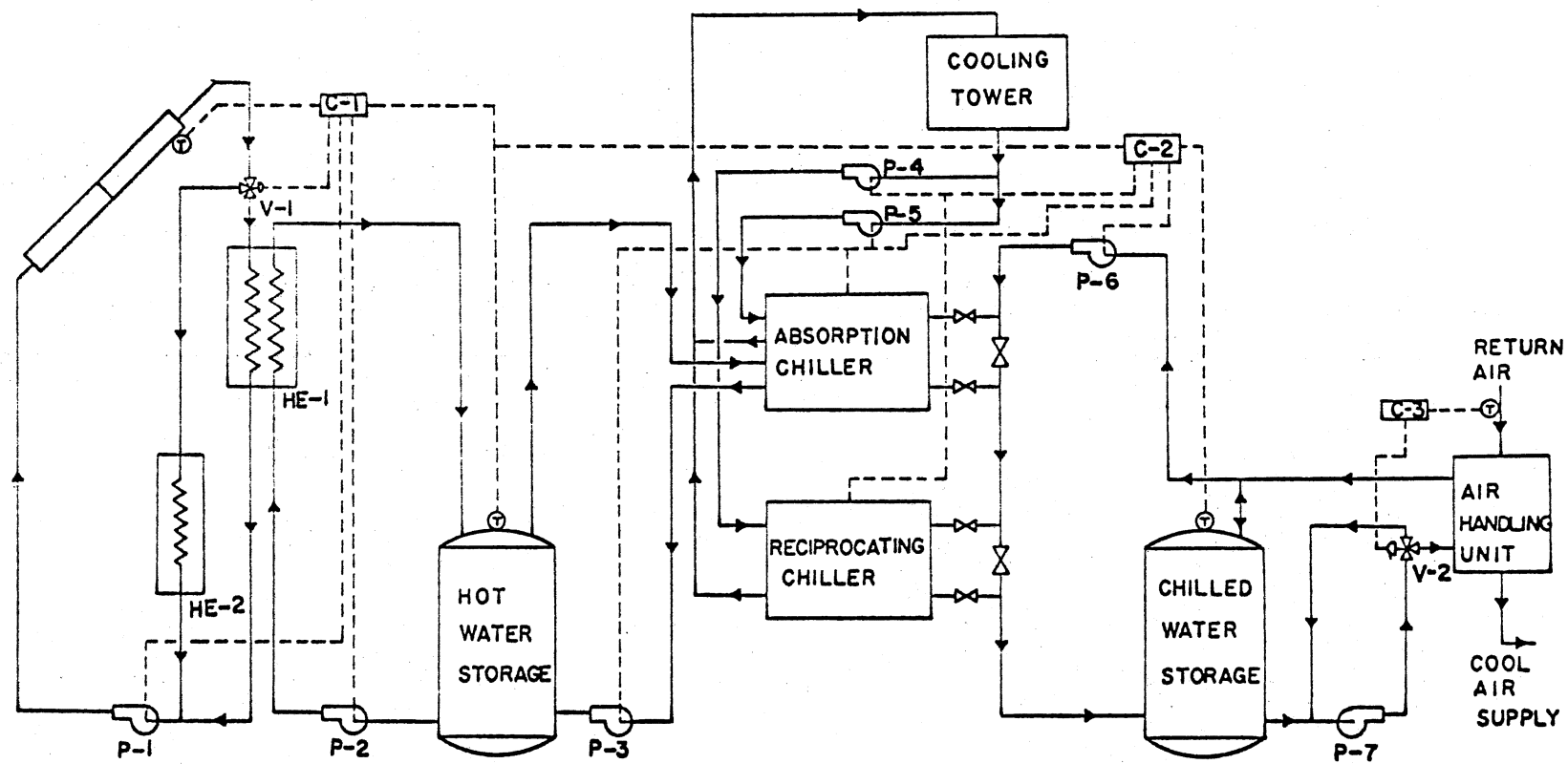
Figure 4. Schematic Diagram of a Solar Cooling System

temperature from the collector is 8°C higher than the hot water temperature, the controller turns on the circulation pumps P-1 and P-2 to start collecting solar energy. When the hot water temperature reaches 95°C and the collector temperature is still higher, the controller turns off pump P-2 and diverts the collector fluid through heat exchanger HE-2 to dissipate the heat to the environment, thus preventing the collector from overheating and the hot storage water from boiling. When the collector outlet temperature is less than 4°C higher than the hot water temperature, both pumps will be turned off and the circulation stopped.

The hot water stored is used to power the absorption chiller when chilling is demanded. The operation of the absorption chiller and the back-up reciprocating chiller is controlled by controller C-2. Controller C-2 senses the temperature of the chilled water and the hot water. When the chilled water temperature is above 9°C and the hot water temperature is higher than 82°C, the controller turns on the absorption chiller to remove heat from the chilled water storage until the chilled water temperature drops to 6°C or the hot water temperature drops below 72°C. If the hot water temperature is not high enough to power the absorption chiller and the chilled water temperature rises above 10°C, the reciprocating chiller will be activated to lower the chilled water temperature to 9°C.

The chilled water delivery pump which delivers chilled water to the air handling unit is controlled by the room thermostat. The amount of chilled water flowing through the air handling unit is controlled by controller C-3 which senses the return air temperature. The unused chilled water is returned to the pump suction. The used chilled water is either returned to the chilled water storage tank when none of the chillers is

operating or mixed with the chilled water drawn from the storage tank
and pumped to the chiller to be chilled and then returned to the storage
tank.

The Simulation Method

A general simulation program for solar energy systems called TRNSYS
(43) was used throughout this study for formulating the simulation model.
Figure 5 is the information flow diagram of the solar cooling system de-
scribed in the previous section. The chilled water circulation sequence
has been rearranged for the sake of modeling simplicity. The rearrange-
ment, however, does not change the basic operating characteristics of
the system.

The driving forces of the solar cooling system are the meteorologi-
cal forces such as solar radiation, wind speed, dry bulb and wet bulb
temperatures. In the simulation process, these forces are introduced by
means of input to the simulation model. These input are in the form of
hourly data measured in or near the location of interest. The solar
radiation used is the global value on a tilted surface facing south with
the tilt angle equal to the latitude of the given location. Usually,
the simulation has to be carried out for a time period on the order of
many years to obtain a sensible indication of the long-term performance
of the system. However, this will require substantial computer time and
hence is not economical. In order to circumvent this, a typical year of
meteorological data was used. Typical meteorological years for 26 SOLMET
stations have been developed by Hall et al. (44). The ability of these
typical meteorological years to predict the long-term performance of
solar systems has been shown to be satisfactory by Freeman (45),
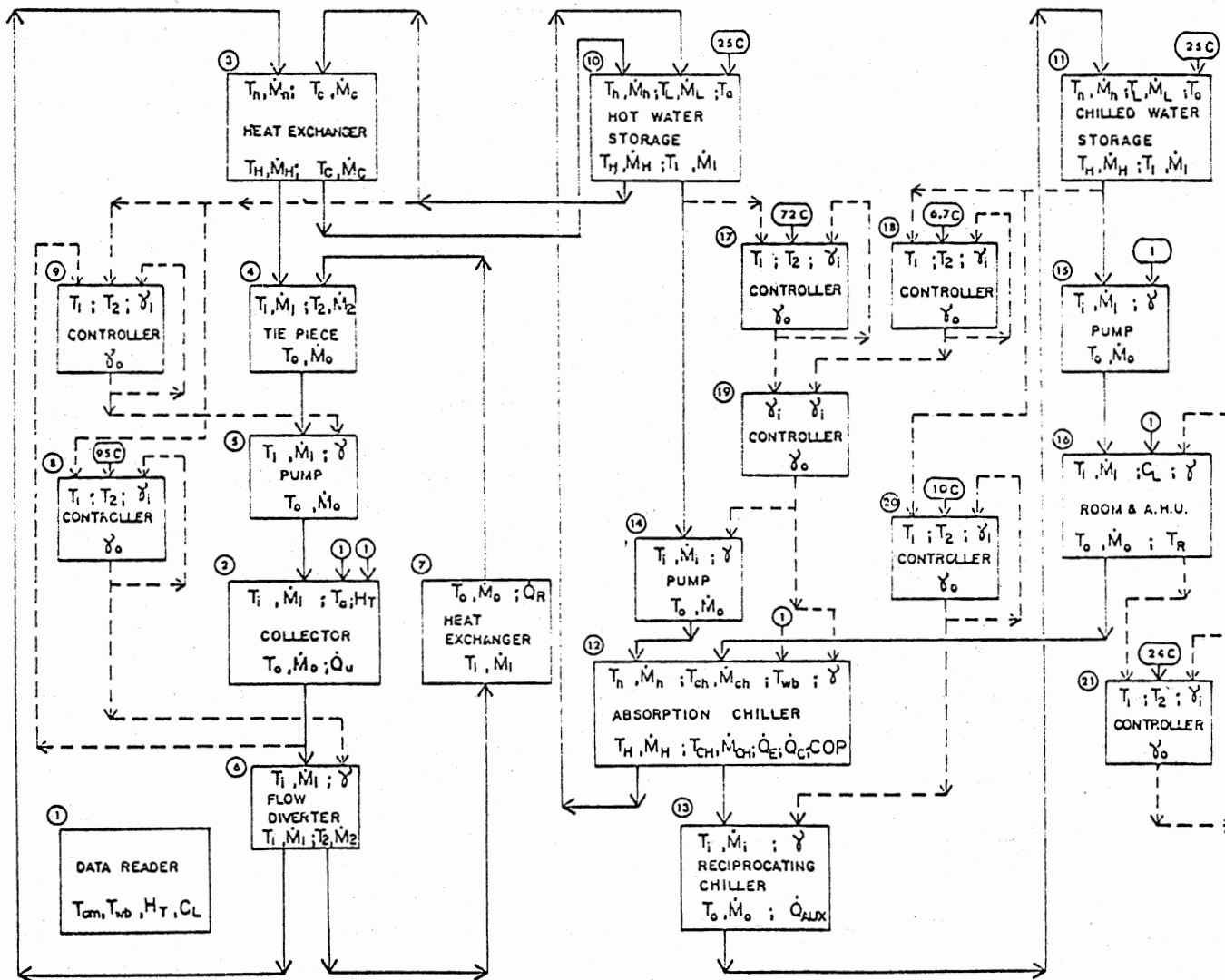
Figure 5.   Information Flow Diagram of the Solar Cooling System Simulation Model

especially in predicting averaged yearly or seasonal performance. In this study the interest was in the performance of the solar cooling system in an averaged cooling season which was defined as consisting of six months, from May to October. Therefore, in the simulation the data of these six months of the typical meteorological year were used.

The cooling load of a building of medium construction was also used as input. A description of the physical parameters of this base building is presented in Appendix A. The simulation model for computing the cooling load of this building was formulated by using TRNSYS which employs the ASHRAE transfer function method. The cooling load was computed for the six months cooling season from May to October using typical meteorological year data of the given location. In order to match the cooling load with the cooling capacity of the absorption chiller used in the system, which has a designed capacity of 25 tons, the cooling load calculated was multiplied by a constant to obtain a peak cooling load equal to 25 tons. The resulting cooling load data were then used repeatedly for all simulations of the system in the same location.

The Component Models

The mathematical models of the system components used in the simulation will be described in this section. Some of the models which have only a small effect on the performance of the system are excluded. The details of these models such as pumps, flow diverters, and controllers can be found in Reference (43). The computer programs of the models that are different from the ones already existing in TRNSYS and the input to the TRNSYS program are listed in Appendix B.

Solar Energy Collector

The collector model employs the Hottel and Whillier collector equation (Equation (3.1)). The collector efficiency factor F', the collector heat removal factor F_R, the collector overall energy loss coefficient U_L, and the transmittance-absorptance product $\tau\alpha$ in the equation are treated as constants. Since selective surface collectors are generally required for solar cooling applications, the typical values for this type of collector were chosen for these four parameters. They are:

$$F' = 0.98$$

$$F_R = 0.94$$

$$\tau\alpha = 0.85$$

$$U_L = 15.0 \text{ KJ/Hr m}^2 \text{ °C}$$

Heat Exchanger

The heat exchanger between the collector and the storage tank is a counterflow heat exchanger. The actual rate of heat transferred $\dot{Q}_{HE}$ can be expressed in terms of the effectiveness of the heat exchanger ε as

$$\dot{Q}_{HE} = \varepsilon C_{min} (T_{h,i} - T_{c,i}) \tag{4.1}$$

where

ε = heat exchanger effectiveness;

C_{min} = minimum capacitance rate;

$T_{h,i}$ = inlet collector fluid temperature; and

$T_{c,i}$ = inlet storage water temperature.

Because the specific heat of the collector fluid is lower than water and the mass flow rates of the two streams are equal, the collector fluid

has the minimum capacitance rate. The outlet collector fluid tempera-
ture and storage water temperature can then be written as

$$T_{h,o} = T_{h,i} - \varepsilon(T_{h,i} - T_{c,i}) \qquad (4.2)$$

$$T_{c,o} = T_{c,i} + \varepsilon \frac{C_h}{C_c} (T_{h,i} - T_{c,i}) \qquad (4.3)$$

where

$T_{h,o}$ = collector fluid outlet temperature;

$T_{c,o}$ = storage water outlet temperature;

C_h = collector fluid capacitance rate; and

C_c = storage water capacitance rate.

The effectiveness of this heat exchanger was assumed to be 0.75.

Storage Tank

The model of the storage tank assumes that the water in the tank is
fully mixed and has a uniform temperature. This assumption ignores the
effect of thermal stratification. Although thermal stratification will
result in nonuniform temperature distribution, its effect on the perform-
ance of solar systems is generally not very large. In addition, a model
that takes into account the thermal stratification will require substan-
tially more computer time for the simulation. Therefore, a fully-mixed
tank model was used. The fully-mixed tank model is described by an
energy balance about the tank which reads:

$$MC_p \frac{dT}{dt} = \dot{Q}_{in} - \dot{Q}_{out} \qquad (4.4)$$

where

M = total mass of storage water;

C_p = specific heat of water;

T = storage water temperature;

$\dot{Q}_{in}$ = rate of total heat transfer into the tank; and

$\dot{Q}_{out}$ = rate of total heat transfer out of the tank.

In the case of hot water storage, $\dot{Q}_{in}$ is the energy collected from the collector; $\dot{Q}_{out}$ is the sum of the heat loss to the environment and the energy supplied to the absorption chiller. For the chilled water storage, $\dot{Q}_{in}$ is the sum of the heat gain from the cooling load and the heat gain from the environment; $\dot{Q}_{out}$ is the heat removed by the chiller.

Absorption Chiller

The absorption chiller was modeled from the performance data for the ARKLA Solaire 300 chiller, which has a design capacity of 25.5 tons. The model expresses the energy input from the heat source $\dot{Q}_h$ and the capacity of the chiller $\dot{Q}_c$ as follows:

For the energy input

$$
\begin{aligned}
\dot{Q}_h = {} & -524245.0 - 76982.3 \, T_h + 213556.0 \, T_s \\
& + 325587.0 \, (T_{\ell,i} - T_{\ell,o}) + 1169.77 \, T_h^2 - 836.132 \, T_s^2 \\
& + 12796.4 \, (T_{\ell,i} - T_{\ell,o})^2 - 2574.89 \, T_h T_s \\
& - 7889.71 \, T_h \, (T_{\ell,i} - T_{\ell,o}) + 8794.59 \, T_s \, (T_{\ell,i} - T_{\ell,o})
\end{aligned}
$$

(4.5)

For the capacity

$$
\dot{Q}_c = \begin{cases} 0 & \text{during the first 15 minutes} \\ 56986.0 \, (T_{\ell,i} - T_{\ell,o}) & \text{after 15 minutes} \end{cases}
$$

(4.6)

$$\dot{m}_h = 19680.0 \text{ Kg/Hr} \tag{4.7}$$

$$\dot{m}_\ell = 13620.0 \text{ Kg/Hr} \tag{4.8}$$

$$\dot{m}_s = 20367.0 \text{ Kg/Hr} \tag{4.9}$$

where

T_h = hot water inlet temperature in degrees C;

T_s = condensing water inlet temperature in degrees C;

$T_{\ell,i}$ = chilled water inlet temperature in degrees C;

$T_{\ell,o}$ = desired chilled water outlet temperature in degrees C;

$\dot{m}_h$ = mass flow rate of the hot water;

$\dot{m}_\ell$ = mass flow rate of the chilled water; and

$\dot{m}_s$ = mass flow rate of the condensing water.

However, for every combination of the hot water inlet temperature, the condensing water inlet temperature and the desired chilled water outlet temperature, there is a maximum inlet chilled water temperature above which the chiller is not able to provide the desired outlet water temperature. This maximum temperature, $T_{\ell,max}$, is expressed as

$$\begin{aligned}
T_{\ell,max} = {} & -51.991 + 0.70636 \ T_h + 1.8395 \ T_s - 0.144089 \ T_{\ell,o} \\
& - 0.0036014 \ T_h^2 - 0.042221 \ T_s^2 - 0.014912 \ T_{\ell,o}^2 \\
& + 0.00112911 \ T_h T_s + 0.00618492 \ T_h T_{\ell,o} \\
& + 0.035438 \ T_s T_{\ell,o}
\end{aligned} \tag{4.10}$$

If the chilled water inlet temperature is higher than $T_{\ell,max}$, the chiller will perform at its maximum capacity which is the capacity when the inlet chilled water temperature equals $T_{\ell,max}$. The energy input and the capacity can be calculated using $T_{\ell,max}$ replacing actual $T_{\ell,i}$. The chilled water outlet temperature in these circumstances is not the desired outlet

temperature but equal to $T_{\ell,o} + (T_{\ell,i} - T_{\ell,max})$. Figures 6 and 7 compare the energy input calculated with the model developed and the ones from the performance data. The modeled values have less than 3 percent error.

Cooling Tower

The cooling tower model assumes constant water and air flow rates. This model is suggested by the ASHRAE task group on energy requirements for heating and cooling of buildings (46). It expresses the temperature of the water leaving the cooling tower as

$$
\begin{aligned}
T_{CW} = {} & 83.4854 - 5.59771\ T_{WB} + 0.115708\ T_{WB}^{2} - 2.03676\ T_{HW} \\
& + 0.00825167\ T_{HW}^{2} + 0.188583\ T_{HW}\ T_{WB} \\
& - 0.00360811\ T_{WB}^{2}\ T_{HW} - 0.000857333\ T_{WB}\ T_{HW}^{2} \\
& + 0.0000180777\ T_{WB}^{2}\ T_{HW}^{2}
\end{aligned}
\tag{4.11}
$$

where

T_{CW} = temperature of water leaving cooling tower in degrees C;

T_{HW} = temperature of water entering cooling tower in degrees C; and

T_{WB} = air wet bulb temperature in degrees C.

The absorption chiller requires the condensing water temperature to be not lower than 24°C. To satisfy this requirement, the air fan of the cooling tower is usually turned off when the water temperature in the sump drops to 24°C to avoid further cooling of the water. Therefore, in the model, if T_{CW} calculated is lower than 24°C, it is made equal to 24°C.
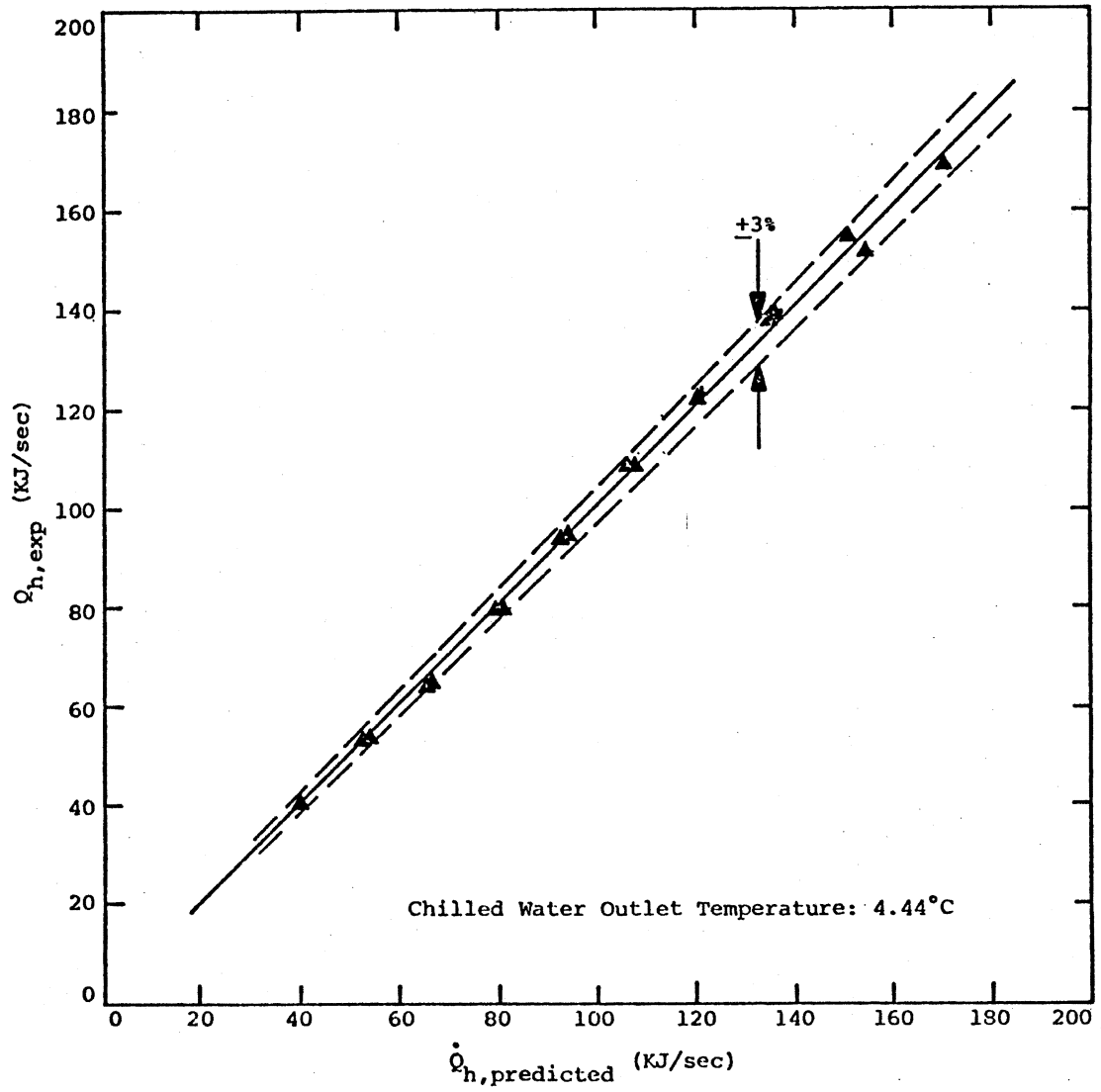
Figure 6. Comparison of the Model Predictions and Experimental
Data for Solaire 300 Chiller (I)
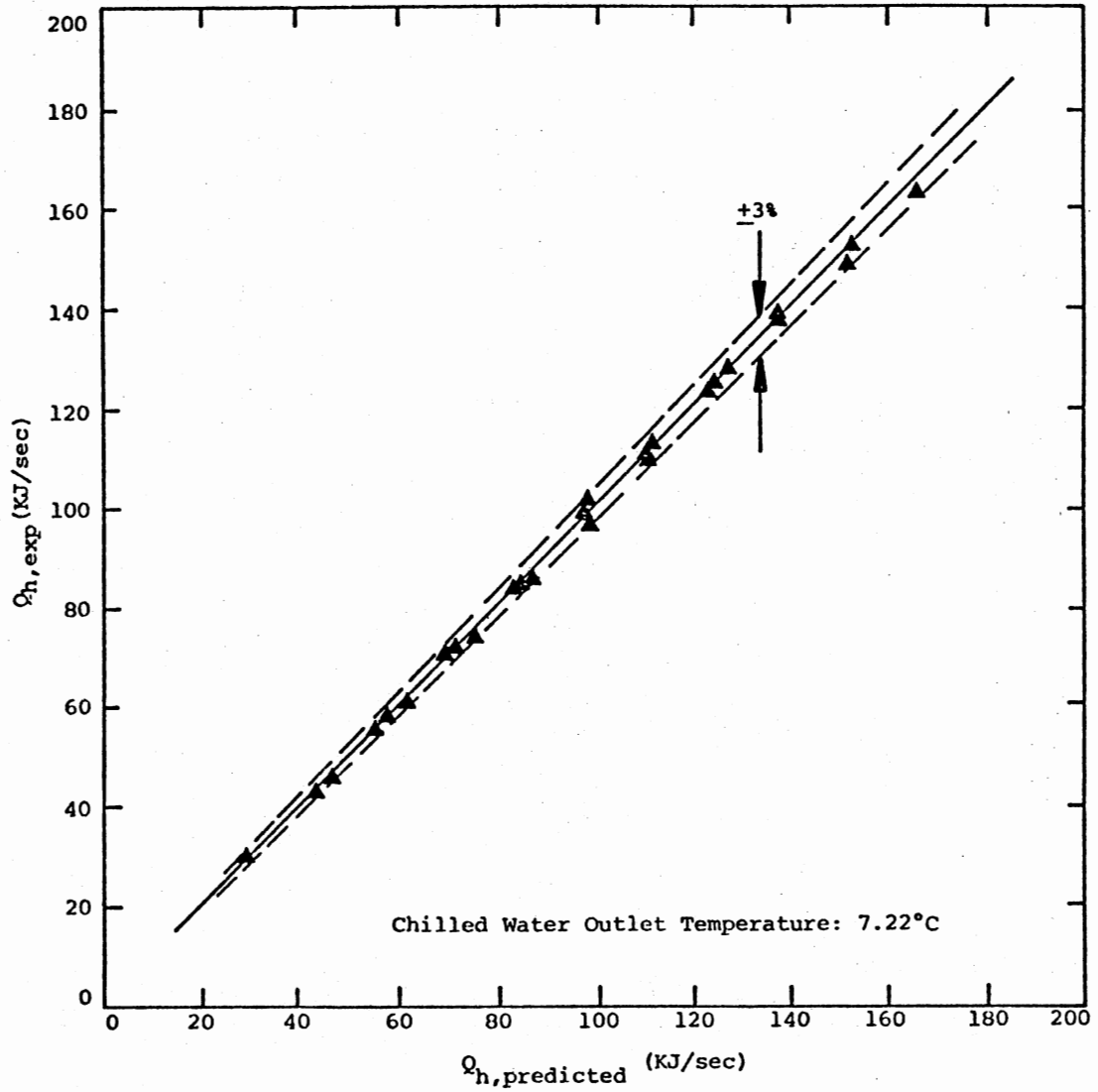
Figure 7. Comparison of Model Predictions and Experimental
Data for Solaire 300 Chiller (II)

Air Handling Unit and Room Air Temperature

The air handling unit removes heat from the conditioned space air. The rate of heat removal from the space, i.e., the heat extraction rate, is a function of the cooling load, air temperature, time, etc. The heat extraction rate can be calculated by using the room air transfer function (47) (48). It is written as

$$\dot{Q}_{x,t} = \frac{g_o}{S + g_o} W_t + \frac{S}{S + g_o} I_t \qquad (4.12)$$

and

$$I_t = T_{rc} \sum_{i=0}^{2} g_i - \sum_{i=1}^{2} g_i T_{r,t-i\Delta} + \sum_{i=0}^{1} p_i \dot{Q}_{L,t-i\Delta} - p_1 \dot{Q}_{x,t-\Delta} \qquad (4.13)$$

$$W_t = \frac{\dot{Q}_{x,max} + \dot{Q}_{x,min}}{2} - ST_r^* \qquad (4.14)$$

$$S = (\dot{Q}_{x,max} - \dot{Q}_{x,min})/\Delta T_r \qquad (4.15)$$

where

g_i, p_i = coefficient of room air transfer function;

$\dot{Q}_{L,t-i\Delta}$ = cooling load at time $t-i\Delta$;

$\dot{Q}_{x,t}$ = heat extraction rate at time t;

$\dot{Q}_{x,t-\Delta}$ = heat extraction rate at time $t-\Delta$;

$\dot{Q}_{x,max}$ = maximum heat extraction rate of air handling unit;

$\dot{Q}_{x,min}$ = minimum heat extraction rate of air handling unit;

$T_{r,t-i\Delta}$ = room air temperature at time $t-i\Delta$;

T_{rc} = constant room temperature used for calculating cooling load;

T_r^* = thermostat set point temperature; and

ΔT_r = throttling range of thermostat.

If the value of $\dot{Q}_{x,t}$ calculated is greater than $\dot{Q}_{x,max}$, it is made equal to $\dot{Q}_{x,max}$; if it is less than $\dot{Q}_{x,min}$, it is made equal to $\dot{Q}_{x,min}$. Then the room air temperature is calculated from the expression:

$$T_{r,t} = \frac{I_t - \dot{Q}_{x,t}}{g_o} \qquad (4.16)$$

The values of the parameters used in this research are as follows:

$\dot{Q}_{x,max}$ = 316305 KJ/Hr = 300,000 BTU/Hr

$\dot{Q}_{x,min}$ = 0 KJ/Hr = 0 BTU/Hr

T_{rc} = 25C = 77°F

T_r^* = 25C = 77°F

ΔT_r = 1.67C = 3°F

g_o = 28827 KJ/Hr°C = 15189.5 BTU/Hr°F

g_1 = -29440 KJ/Hr°C = -15512.4 BTU/Hr°F

g_2 = 1106.4 KJ/Hr°C = 582.96 BTU/Hr°F

p_o = 1.0

p_1 = -0.87

Simulation Results

The typical meteorological year data for Dodge City, Kansas, and Fort Worth, Texas, were chosen for studying the effect of the sizes of the chilled water storage, hot water storage, and collector area on the performance of the solar cooling system. The seasonal total solar radiation falling on a unit area of the collector in Dodge City is larger than that in Fort Worth: 4.46×10^6 KJ/m^2 in Dodge City and 3.89×10^6 KJ/m^2

in Fort Worth. The seasonal total cooling load of the base building
used in this study, however, is higher in Fort Worth than in Dodge City.
They are 4.094 x 10^8 KJ and 3.458 x 10^8 KJ, respectively.

The effects of the size of the chilled water storage are plotted in
Figures 8 and 9. The solar fraction is defined as the fraction of the
total cooling load that is supplied by the solar energy source. The sys-
tem without chilled water storage, i.e., chilled water storage volume
equal to zero, has a system configuration slightly different than the
system with chilled water storage. It also uses a different control
strategy in that the chillers are controlled by the room air temperature
and not by the chilled water storage tank temperature. The dashed lines
in the figure between chilled water storage volume equal to 0 m^3 and
10 m^3 are to suggest this change of the system configuration and control
strategy. The effect of the size of the chilled water storage is evident
in both figures. The COP of the system with 40 m^3 chilled water storage
volume is about 60 percent higher than the COP of the system without
chilled water storage in Dodge City and about 30 percent higher in
Fort Worth. The solar fraction of the former system is about 47 percent
higher than the solar fraction of the latter system in Dodge City and 25
percent higher in Fort Worth. There are three important characteristics
in the figures worth discussing. First, the slope of the curves, which
levels off when chilled water storage volume is near 40 m^3, suggests a
maximum of both the COP and the solar fraction in this region. Second,
the COP of the system is higher in Fort Worth, Figure 9, than in Dodge
City, Figure 8. On the contrary, the solar fraction is lower in Fort
Worth. This reflects the relative values of the solar radiation and the
cooling load in the two locations. In Fort Worth, the higher cooling

Figure 8. Simulation Results of the Solar Cooling
System With Various Chilled Water
Storage Volumes for the Base Building
in Dodge City, Kansas
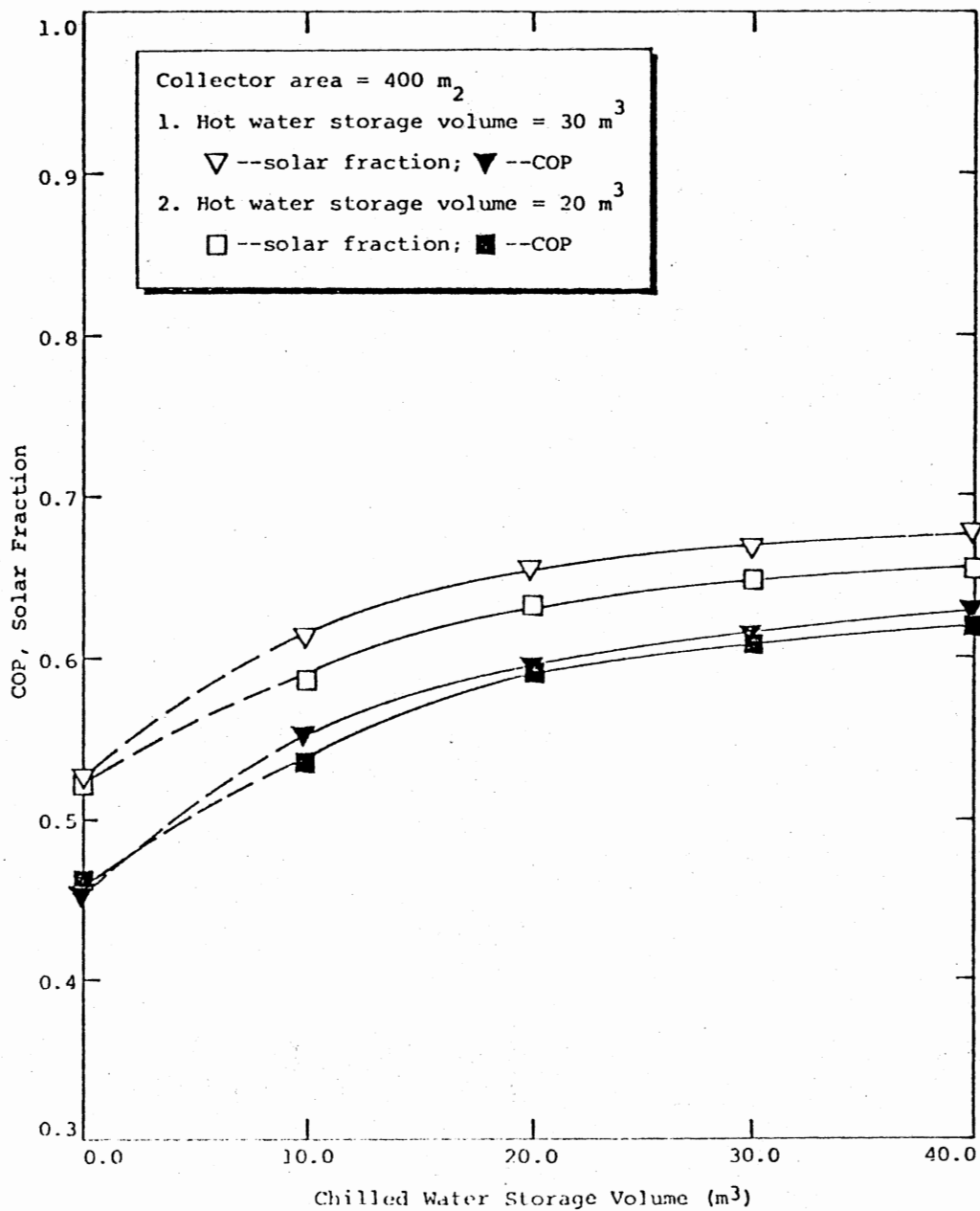
Figure 9. Simulation Results of the Solar Cooling
System With Various Chilled Water
Storage Volumes for the Base Building
in Fort Worth, Texas

load causes the chiller to work more continuously and hence has a higher COP. However, the lower solar radiation and higher cooling load together make the solar fraction low. Third, the slope of the curves for Dodge City is greater than the slope of the curves for Fort Worth. This shows that the size of the chilled water storage is more important in the location where the ratio of the available solar energy to the cooling load is higher.

In Figures 10 and 11 are the performance of the system with various sizes of the hot water storage. The effect of size of the hot water storage on the COP is relatively small. However, its effect on the solar fraction is quite large. The solar fraction of a system with 40 m^3 hot water storage is about 22 percent higher than that of a system with only 10 m^3 hot water storage in Dodge City and about 18 percent higher in Fort Worth. The three characteristics mentioned in the previous section, namely the existence of maximum for the solar fraction and the COP, the higher COP and lower solar fraction in Fort Worth, and the greater slope of the curves for the COP and the solar fraction in Dodge City are also observed in Figures 10 and 11.

The effect of the collector size on the performance of the cooling system can be found in Figure 12. Understandably, the solar fraction of the system increases with the collector size. However, the COP of the absorption chiller is inversely proportional to the collector area. The COP curves in Figure 12 bear a remarkable resemblance to the COP curves in Figures 10 and 11. The only difference is the sign of their slope in that the slope of the curves is negative in Figure 12 and is positive in Figures 10 and 11. This points out an important fact: increasing the collector area has the same effect on the COP of the absorption chiller
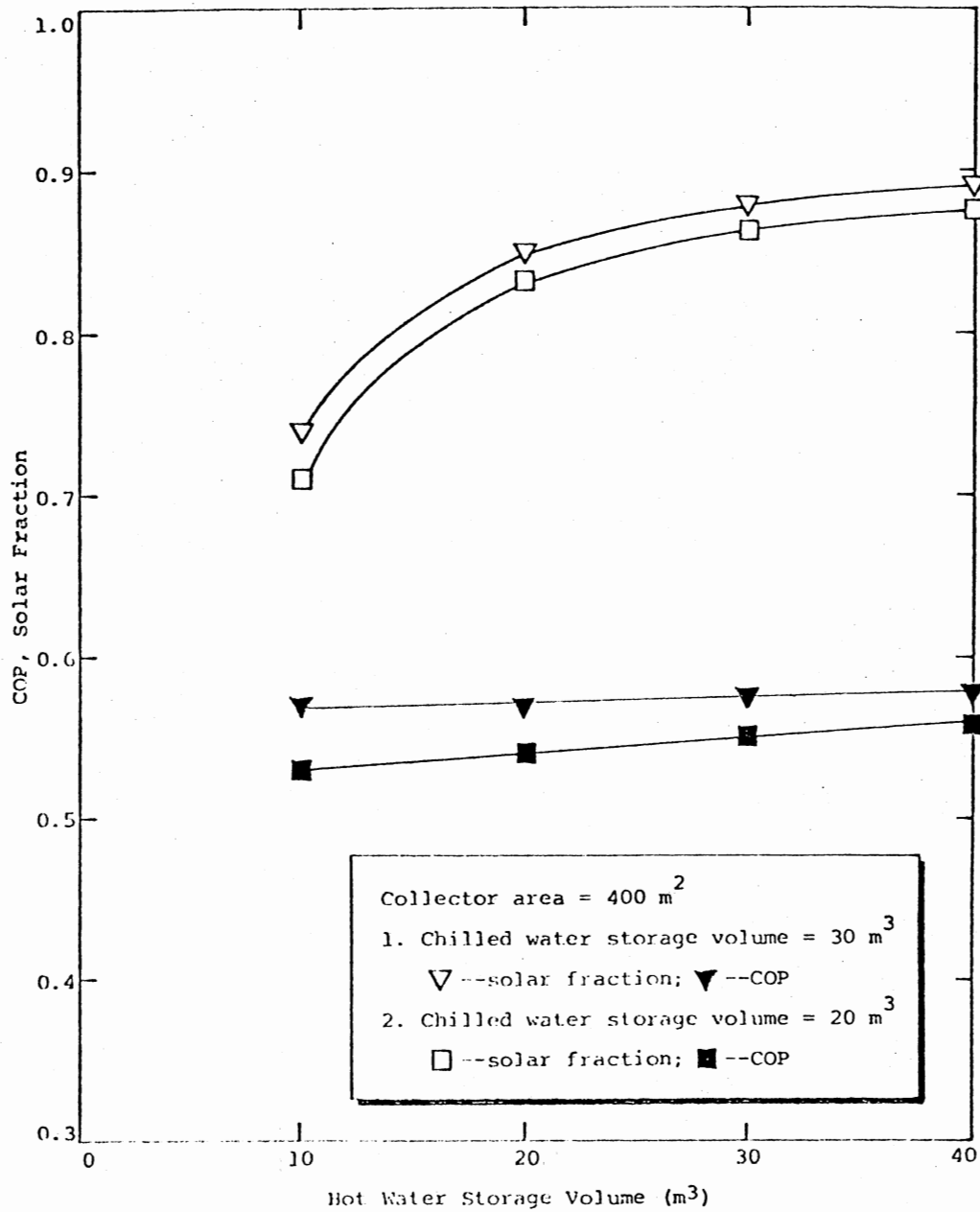
Figure 10. Simulation Results of the Solar Cooling System
With Various Hot Water Storage Volumes for
the Base Building in Dodge City, Kansas
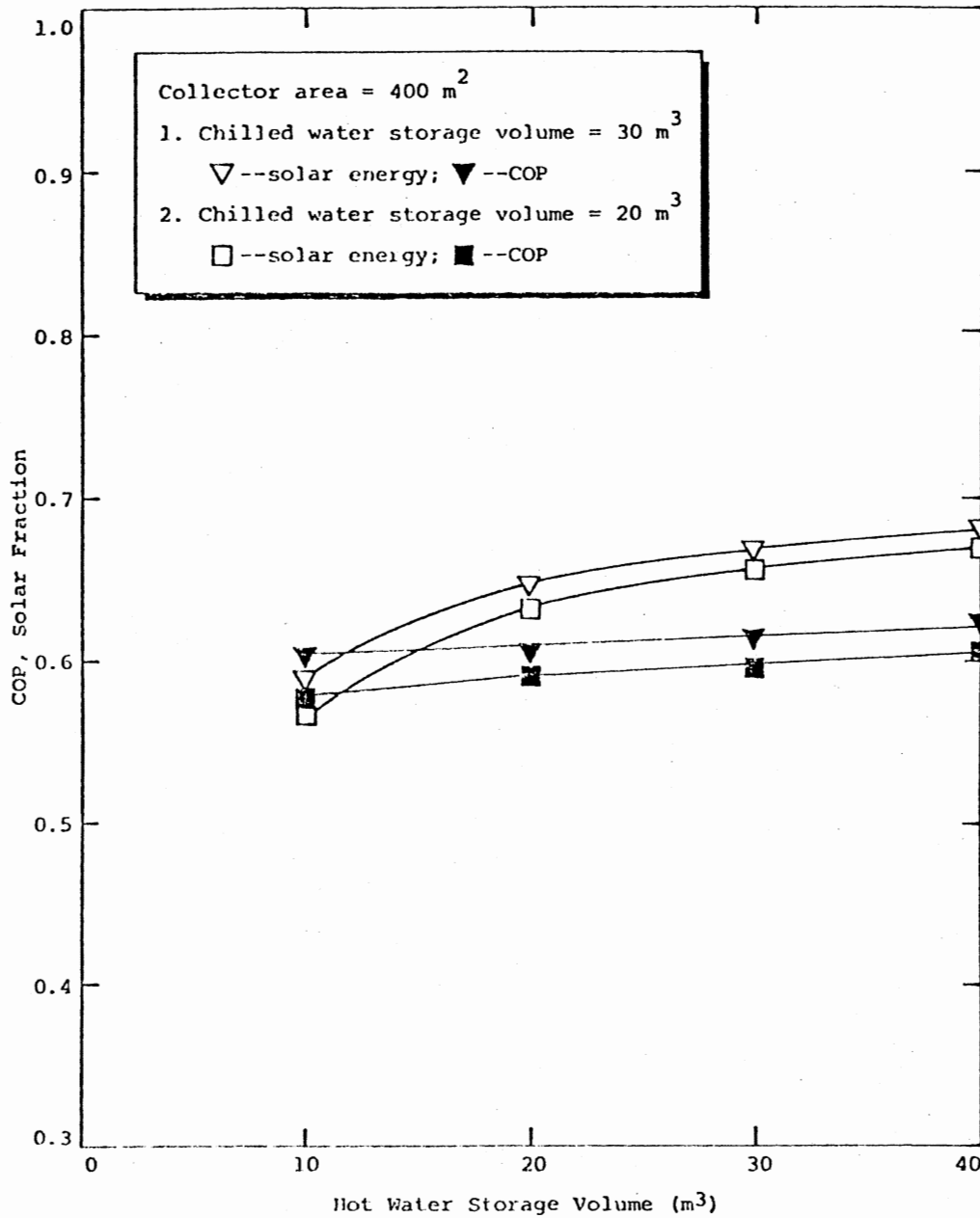
Figure 11.   Simulation Results of the Solar Cooling System
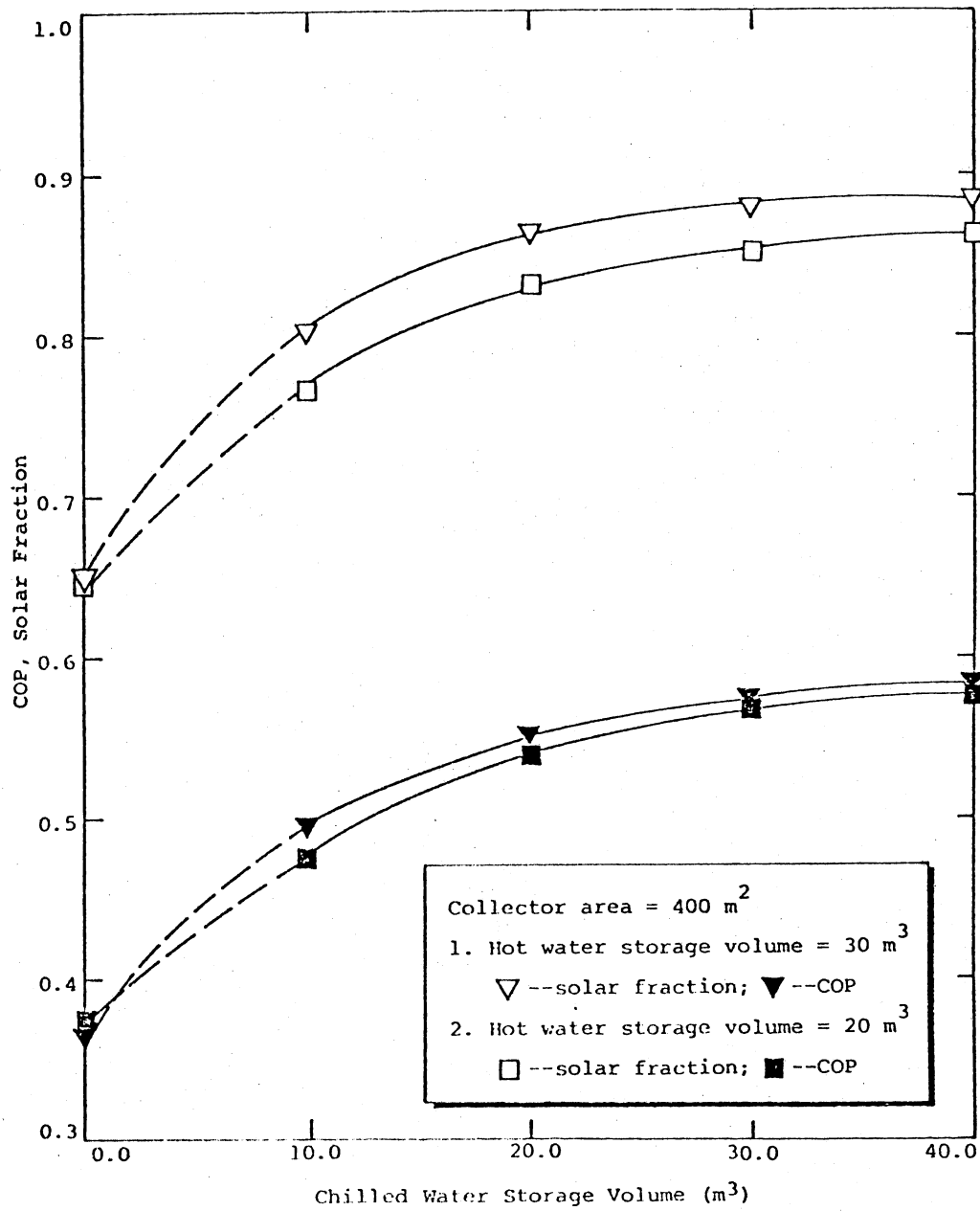With Various Hot Water Storage Volumes for
the Base Building in Fort Worth, Texas
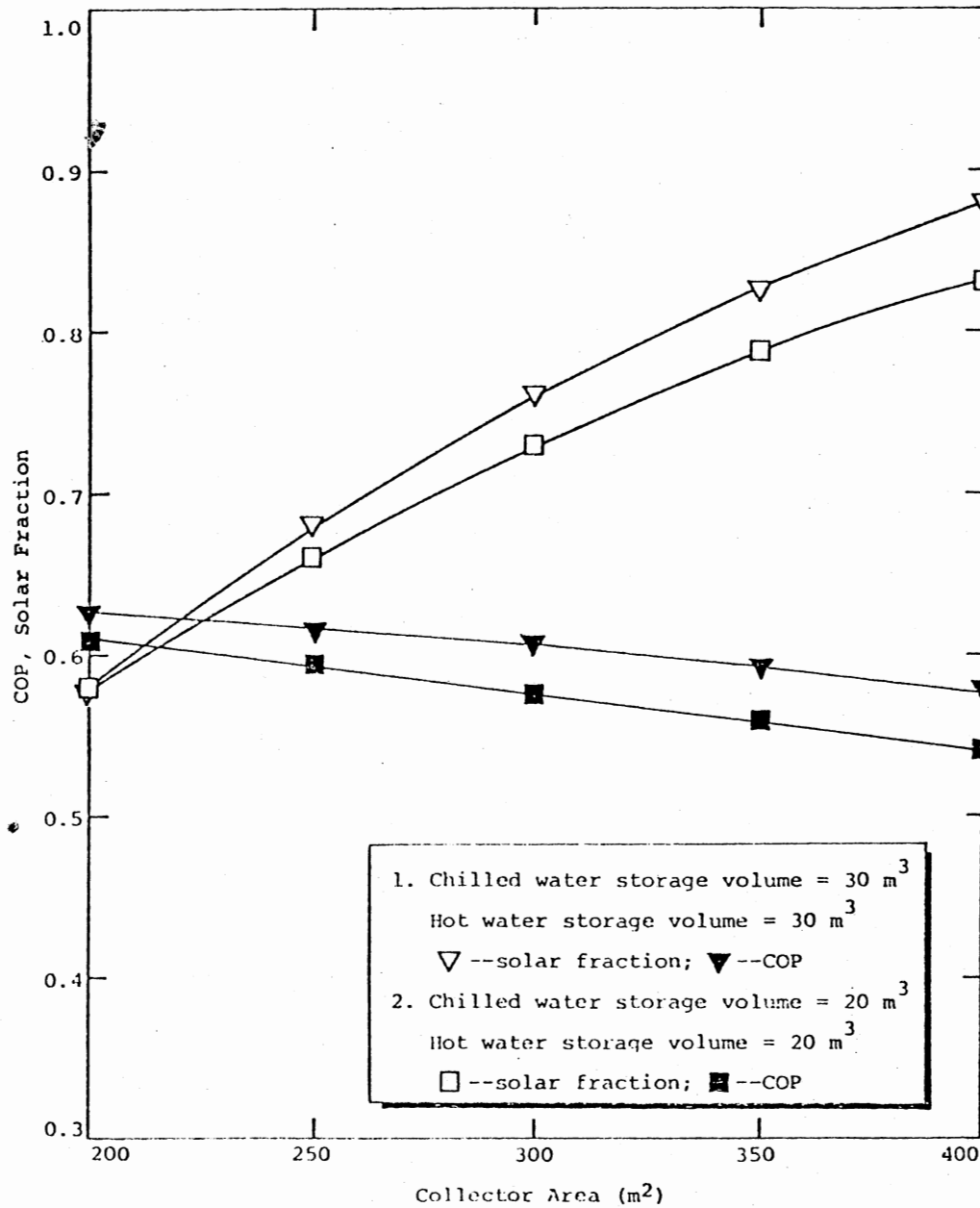
Figure 12. Simulation Results of the Solar Cooling
System With Various Collector Areas
for the Base Building in Dodge City,
Kansas

as decreasing the hot water storage volume. Properly balancing the

sizes of the collector area and the hot water storage volume, therefore,

is very important for improving the system performance.

CHAPTER V

DERIVATION OF A SEMI-EMPIRICAL EQUATION FOR THE

PERFORMANCE OF SOLAR COOLING SYSTEMS

WITH CHILLED WATER STORAGE

A simulation model is a very useful tool for the design of solar cooling systems. However, for designers who do not have access to computer facilities, it is not a practical method. In addition, using simulations to design solar cooling systems is often repetitious and time consuming, especially when optimizing a system which requires evaluating the system performance numerous times to obtain an optimum design. For these reasons it is desirable to develop a simpler method for evaluating the performance of solar cooling systems. In this chapter the approach used to derive a semi-empirical equation for predicting the performance of solar cooling systems with chilled water storage will be described. The term "semi-empirical" refers to the fact that the data used to derive the equation are generated by simulations instead of actual experiments.

Selection of Parameters

An empirical equation is developed by statistically correlating the performance data and the significant parameters of the system. Finding an accurate correlation depends to a large extent on the proper selection of the parameters. The selection of parameters is generally done by

sensitivity analyses. The simulation described in Chapter IV can be used for this purpose.

In Chapter IV, the sizes of the chilled water storage, the hot water storage, and the collector area were found to have significant effects on the performance of solar cooling systems. In addition, the cooling load and the meteorological conditions, notably the solar radiation, the dry bulb and wet bulb temperatures, were also found to be important parameters. Generally speaking, the efficiency of the solar energy collector is also an important factor. However, the collectors suitable for solar cooling applications are limited to high efficiency collectors. Therefore, the difference in the collector efficiency for solar cooling systems is not large and can be excluded from the equation.

The seven parameters selected were grouped into four dimensionless parameters. They are:

$$V_H^* \equiv \frac{\rho\, V_H\, C_p\, \Delta T_H}{S\, A_c/N} \tag{5.1}$$

$$V_C^* \equiv \frac{\rho\, V_C\, C_p\, \Delta T_C}{L/N} \tag{5.2}$$

$$T^* \equiv \frac{\overline{T}_{DB} - \overline{T}_{WB}}{\overline{T}_{DB}} \tag{5.3}$$

$$A_C^* \equiv \frac{S\, A_C}{L} \tag{5.4}$$

where

ρ = density of water;

V_H = hot water storage volume;

V_C = chilled water storage volume;

ΔT_H = hot water temperature variation range;

ΔT_C = chilled water temperature variation range;

C_p = specific heat of water;

A_c = collector area;

S = seasonal total solar radiation incident on the solar collector surface per unit collector area;

L = seasonal total cooling load;

N = number of days in the cooling season;

$\overline{T}_{DB}$ = design dry bulb temperature in absolute units; and

$\overline{T}_{WB}$ = mean coincident wet bulb temperature of the design dry bulb temperature in absolute units.

The design dry bulb temperature and its mean coincident wet bulb temperature can be found in the ASHRAE Handbook of Fundamentals (49). The values used here were the 2.5 percent design values, which means that in only 2.5 percent of the total hours in the cooling season the dry bulb temperature is expected to be equal or above the design value. The products $\rho V_H C_p \Delta T_H$ in Equation (5.1) and $\rho V_C C_p \Delta T_C$ in Equation (5.2) are the hot water storage thermal capacity and the chilled water storage thermal capacity, respectively.

Method of Generating Performance Data

Generating the performance data is another important step in developing an empirical equation. The performance data should provide as much information about the performance characteristics of the solar cooling system as possible. Usually the amount of information is proportional to the amount of performance data; however, so is the computer time required to generate the data. Therefore, a carefully planned method of

generating performance data was necessary to gain a maximum amount of information with a minimum number of computer simulations.

Among the seven parameters selected in the previous section, the seasonal total solar radiation, the design dry bulb and wet bulb temperatures, and the cooling load are weather and location dependent. If the typical meteorological year data were used, these four parameters will be constants for a given location, that is, they become location dependent. To obtain enough variations of these four parameters, the typical meteorological year data of several locations had to be used in the simulations. Seven out of the twenty-six SOLMET stations, which have typical meteorological year data available, were chosen for this purpose. These seven locations have sufficient diversification in their weather patterns to provide enough variations of the four location dependent parameters. The value of these four parameters for the seven locations chosen are listed in Table I.

The other three parameters, namely the sizes of the chilled water storage, the hot water storage, and the collector area, are design parameters. These three parameters are the ones that can be varied for a solar cooling system in a given location. The ranges of these three parameters condidered were between 240 m^2 and 440 m^2 for the collector area and between 10 m^3 and 40 m^3 for both the chilled water and the hot water storage volume. The performance of the solar cooling system with different combinations of the values of these three parameters is the information desired. For generating the performance data, six values within the range considered were chosen for each of the three parameters. However, to simulate the solar cooling system with every combination of the six values of these three parameters would require 216 simulations, which

TABLE I

THE VALUES OF THE LOCATION DEPENDENT PARAMETERS
FOR THE SEVEN LOCATIONS CHOSEN

Location	Total Seasonal Insolation $(KJ/Hr-m^2)$ x 10^{-6}	Total Seasonal Cooling Load (KJ) x 10^{-6}	Design Dry Bulb Temperature ($2\frac{1}{2}$% Value) (°C)	Coincident Wet Bulb Temperature (°C)	Latitude
Dodge City, Kansas	4.45635	345.822	36.11	20.56	37° 5'
Fort Worth, Texas	3.89172	450.562	37.22	23.33	32° 5'
El Paso, Texas	4.69030	409.964	36.67	17.78	31° 5'
Albuquerque, New Mexico	4.58162	292.778	34.44	16.11	35°
Columbia, Missouri	3.87053	320.989	34.44	23.33	39°
Nashville, Tennessee	3.61883	396.382	34.44	23.33	36° 1'
Lake Charles, Louisiana	3.46762	457.944	33.89	25.00	30° 1'

is a formidable task. To reduce the number of simulations required, a factorial plan was used (50) (51). The factorial plan with the six values used for the three parameters is shown in Figure 13. The number Of simulations is reduced to 36. The performance data resulting from these 36 simulations can provide sufficient information about the system performance characteristics, because each value of one parameter has been combined once with every value of the other two parameters. These 36 simulations were carried out using the typical meteorological year data for Dodge City, Kansas. But for the rest of the seven locations, only 10 of the 36 simulations were performed for each location. The reason for this is twofold. First, if 36 simulations were performed for each of the seven locations, the number of simulations would become too large. Second, the purpose of simulating the solar cooling system at different locations was to consider the variations of the four location dependent parameters. The variations of the three design parameters are less important in the last six locations, since the effect of the variations of these three parameters have already been fully considered in the first location. Nevertheless, the 10 simulations performed in each of the last six locations were carefully chosen so as to distribute evenly among the six values of the three design parameters. In addition, the way of arranging the factorial plan and the values for the three parameters were changed in some locations to avoid combining the values of the three parameters in a fixed fashion. The performance data resulting from these simulations can be found in Appendix C.

Formulation of the Semi-Empirical Equation

Formulating the empirical equation was a difficult step, because

Collector Area (m²)	Hot Water Storage Volume (m³)					
	10	2ʊ	25	30	35	40
Chilled Water Storage Volume (m³) 40	(1) 240	(2) 280	(3) 320	(4) 360	(5) 400	(6) 440
35	(7) 280	(8) 320	(9) 360	(10) 400	(11) 440	(12) 240
30	(13) 320	(14) 360	(15) 400	(16) 440	(17) 240	(18) 280
25	(19) 360	(20) 400	(21) 440	(21) 240	(22) 280	(24) 320
20	(25) 400	(26) 440	(27) 240	(28) 280	(29) 320	(30) 360
10	(31) 440	(32) 240	(33) 280	(34) 320	(35) 360	(36) 400

Figure 13. Factorial Plan for Selecting the Sizes of
the Hot Water Storage Volume, Chilled
Water Storage Volume, and Collector Area

there is no methodical procedure for selecting the form of the equation.
In general, some helpful information can be obtained by plotting the
performance data versus the parameters. However, in most cases, intui-
tion is often required in sensing the form of the equation to be used.

The objective of the semi-empirical equation is to express the
solar fraction SF in terms of the four dimensionless parameters derived
previously, i.e., V_H^*, V_C^*, T^*, and A_C^*. The equation is expected to have
the following form:

$$SF = f_1(A_C^*) \; f_2(T^*) \; f_3(V_H^*, V_C^*) \tag{5.5}$$

The functions f_1, f_2, and f_3 may be any type of functions such as poly-
nomials or exponentials. If the exponential forms were used, these
three functions can be written as

$$f_1(A_C^*) = A_C^{*\,a_1} \tag{5.6}$$

$$f_2(T^*) = T^{*\,a_2} \tag{5.7}$$

$$f_3(V_H^*, V_C^*) = a_3 + a_4 \, V_H^{*\,a_5} + a_6 \, V_C^{*\,a_7} + a_8 \, (V_H^*, V_C^*)^{a_9} \tag{5.8}$$

where the a's are the coefficients to be determined.

So far, the equation is only a tentative equation. The success of
the equation is judged by how well the equation is able to fit the per-
formance data. One definition of the goodness of fit is the sum of the
squares of the deviation from the data point. The problem then is re-
duced to whether there exists a set of coefficients that enable the equa-
tion to have a sum of the squares of the deviation within an acceptable
tolerance. A computer program called MARQ, developed by Chandler and

Jackson (52), was used for this purpose. This program performs a non-linear least squares fit of a user-supplied function to a given set of data, using the Marquardt-S method, or the Gauss-Newton method, or a modified Gauss-Newton method. If the least squares fit could produce a set of coefficients with acceptable goodness of fit, the equation will be used. Otherwise, a new equation will be formulated and examined.

The form of Equation (5.5), after several trials, was modified to become

$$SF = f_1(A_C^*) \; [f_2(T^*) + f_3(V_H^*, V_C^*)] \tag{5.9}$$

where

$$f_1(A_C^*) = A_C^{*a_1} \tag{5.10}$$

$$f_2(T^*) = a_2 \, T^{*a_3} \tag{5.11}$$

$$f_3(V_H^*, V_C^*) = a_4 \, V_H^{*a_5} + a_6 \, V_C^{*a_7} + a_8 \, (V_H^* \, V_C^*)^{a_9} \tag{5.12}$$

The coefficients were determined by using MARQ and the sum of the squares of the deviation from the performance data generated in the previous section was found to be within acceptable tolerance. The final form of the equation was

$$SF = A_C^{*0.531963} \; [3.39978 \, T^{*1.1018} - 0.144995 \, V_H^{*1.29191}$$

$$+ \, 0.516818 \, V_C^{*-0.063994} - 0.179522 \, (V_H^* \, V_C^*)^{-0.195043}] \tag{5.13}$$

The comparison of the equation predictions and some performance data of the seven locations selected are shown in Figures 14 and 15. Most of
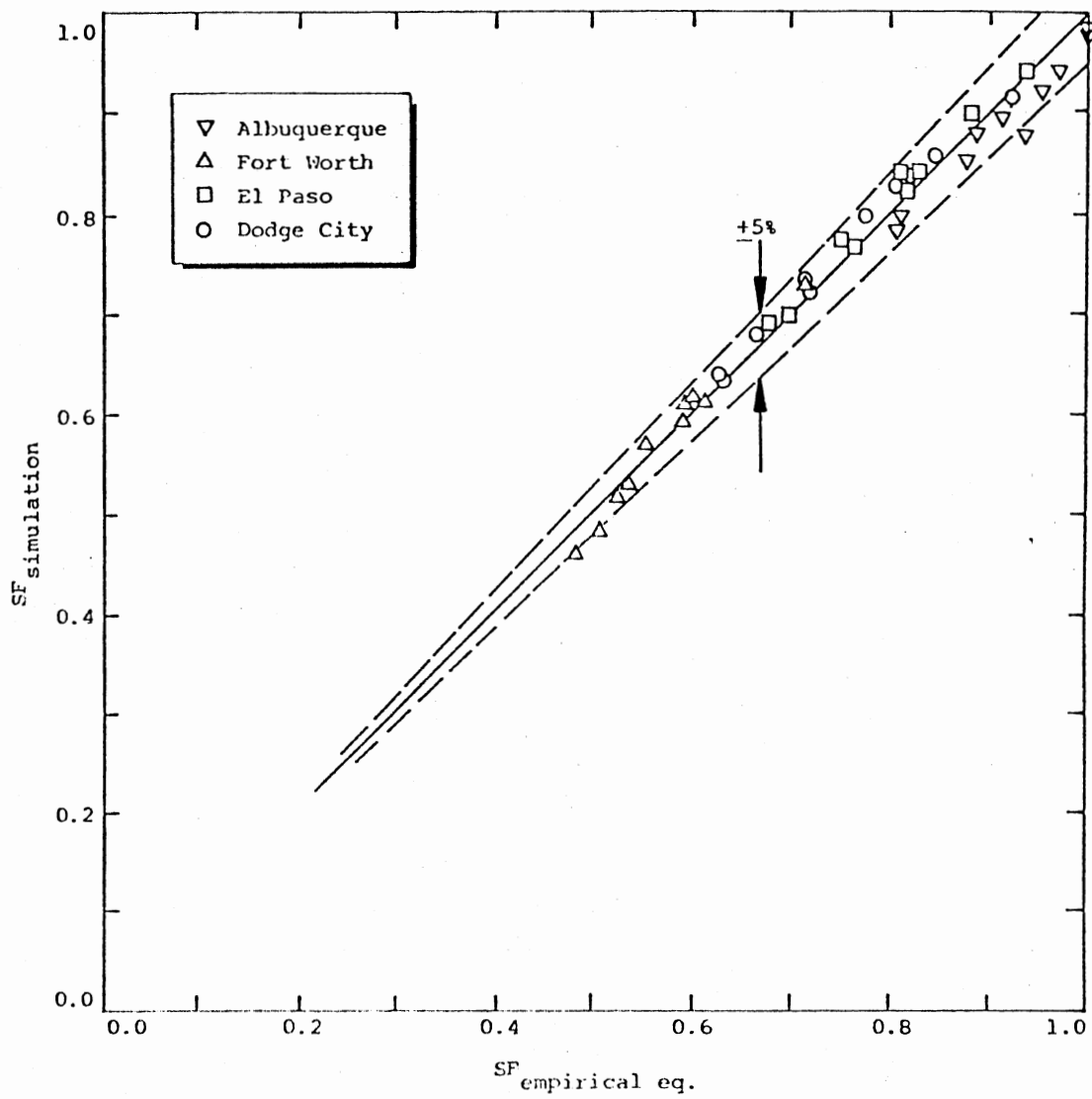
Figure 14. Comparison of the Empirical Equation
Predictions With the Simulation
Results (I)
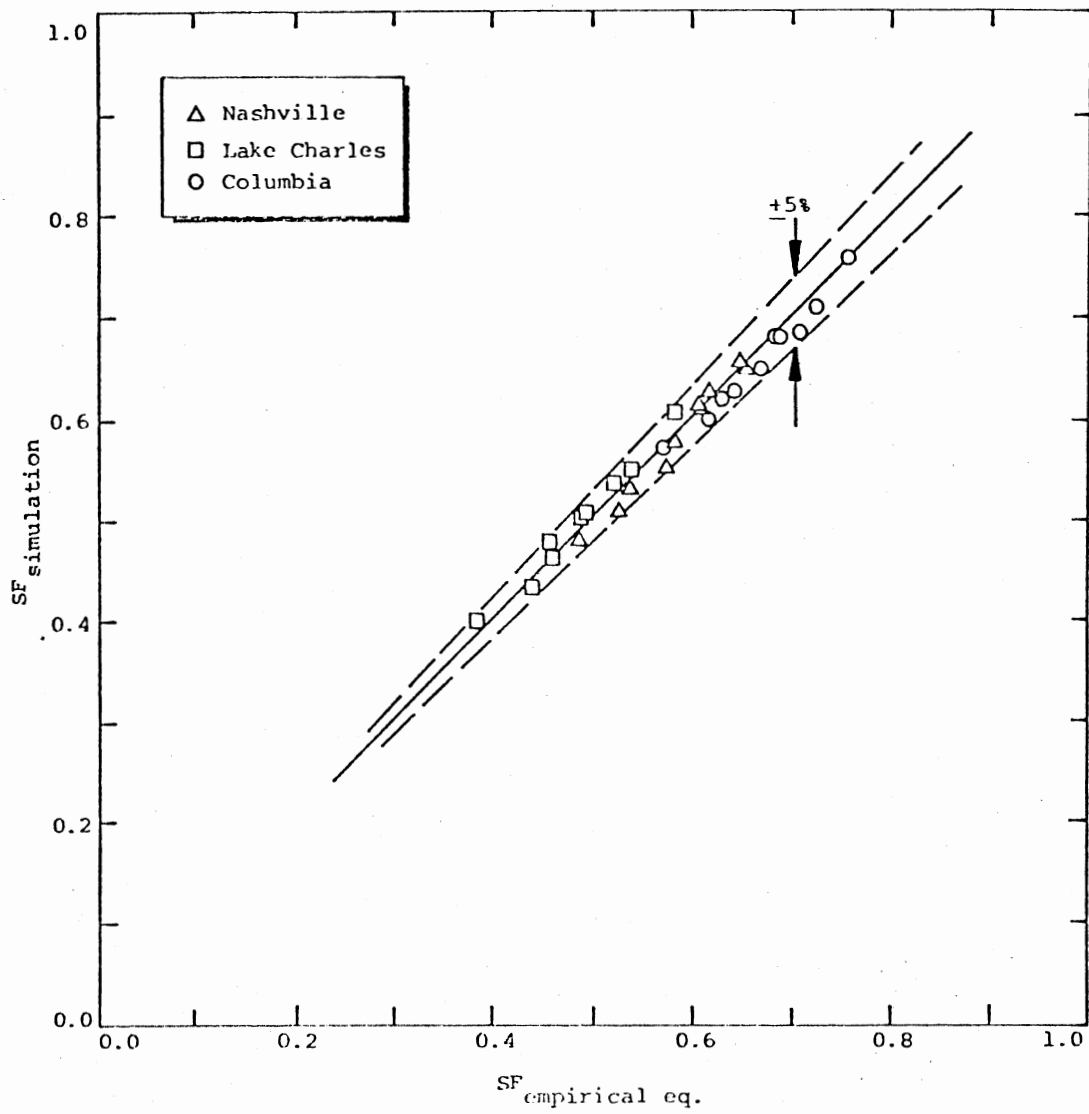
Figure 15. Comparison of the Empirical Equation
Predictions With the Simulation
Results (II)

the equation predictions have less than five percent error. Only 3 of the 96 predictions have errors between five and six percent.

There are two limitations of this equation. First, the equation was derived from simulation results using typical meteorological year data; therefore, it should be used only to predict the long-term averaged seasonal performance. Second, the ranges of the component size are limited to between 240 m^2 and 440 m^2 for the collector and between 10 m^3 and 40 m^3 for both the chilled water storage volume and the hot water storage volume. Although equation predictions of the performance of systems with only 200 m^2 collector area were found to have less than five percent error, using the equation to predict the performance of systems with component sizes which differ too much from these ranges is not recommended. On the other hand, a system with reasonably sized components should be well within the ranges covered.

CHAPTER VI

ECONOMICAL ASPECTS AND OPTIMIZATION OF

SOLAR COOLING SYSTEMS

Economical feasibility is, in most cases, an important criterion for
determining the practicability of solar cooling systems. The basic econo-
mical consideration concerning a solar cooling system is the total cost
of the system versus the cost of the fuel saved during the expected life-
time of the system. Often the objective is to optimize the trade-off be-
tween the total cost of the system and the cost of fuel saved. In this
chapter the significant cost parameters of solar cooling systems will be
discussed first. Then a method for life cycle cost analysis will be de-
scribed. Finally, a general procedure for obtaining an economical opti-
mal system design will be presented.

Significant Cost Parameters

The total cost of a solar cooling system can generally be categorized
as the costs of owning and the costs of operating the system. The costs
of owning a solar cooling system are the costs associated with the ini-
tial investment, that is, the interest on the investment and its repay-
ment over a specified number of years related to its lifetime. The ini-
tial investment, however, should only include the costs of items that are
not normally part of a conventional system, such as the costs of the col-
lector, the absorption chiller, cooling tower, storage tanks, and

associated controls, pumps, pipes, etc. Among these, some costs vary according to the size of the components, while others are relatively fixed. For example, the costs of the collector and storage tanks are size-dependent. On the other hand, the cost of the control system is largely independent of the system size. For simplicity of estimating the initial investment, the costs of the components were classified into three categories. The first category includes the costs that are proportional to the size of the collector. These are the costs of the collector, its support structure, the circulation pumps and pipes, and heat exchangers. The sizes of these components all have to be designed according to the size of the collector; therefore, the costs of these items are proportional to the size of the collector. The second category includes the costs that are proportional to the sizes of the storage tanks. These are the costs of storage tanks, the necessary insulation materials, and support structures. The third category includes the costs that are independent of the sizes of either the collector or storage tanks. These costs are usually fixed for a given application. The costs of the control system, cooling tower, absorption chiller, and associated pumps and pipes are in this category. The initial investment of a solar cooling system then can be expressed as:

$$P = C_A A_C + C_S V_S + C_E \qquad (6.1)$$

where

P = initial investment;

C_A = total cost of first category components per unit collector area;

A_C = collector area;

C_S = total cost of second category components per unit storage

tank volume;

V_S = total storage tank volume; and

C_E = total cost of third category components.

The operating costs are the costs of the power requirements for the circulation pumps and the maintenance costs. Maintenance costs include repairs, replacement of glass in collectors, or any other costs of keeping the system in operating condition. Generally, the annual maintenance costs are proportional to the size of the system and usually amount to about one percent of the initial investment, while the annual pumping costs are on the order of one-tenth of the maintenance costs. Therefore, the total annual operating costs are often estimated as a fixed percentage of the initial investment with one percent of the initial investment being used most often (53).

Life Cycle Cost Analysis: Annual Cost Method

A life cycle cost analysis is the most used means for making economic evaluations of solar cooling systems. There are four life cycle cost analyzing methods, namely the present worth method, the rate of return method, the number of years to break even method, and the annual cost method (54). The annual cost method was adapted in this study because it is more natural for most people to think in terms of annual cost than in terms of the present worth or other methods of comparison.

The annual cost method translates all nonannual costs to an annual cost basis. For the costs of a solar cooling system, the operating costs are already in the annual cost basis, that is, the annual operating costs are estimated to be about one percent of the initial investment,

whereas the owning costs and the cost of fuel saved are not in annual cost basis and need to be translated.

The owning costs include the initial investment and its interest. If the initial investment is to be repaid with equal annual payments over a specified number of years, which usually is equal to the expected system lifetime, and the interest is charged on the amount that is not yet repaid and is compounded annually, the annual payment can be considered as the annual cost of ownership. It can be expressed in terms of the initial investment, the interest rate, and the number of years for the repayment as:

$$R = [\frac{i(1 + i)^n}{(1 + i)^n - 1}] P \tag{6.2}$$

where

R = annual cost or annual payment;

P = initial investment or principle;

i = interest rate; and

n = number of years for the repayment.

The first term on the right is the capital recovery factor which is used to translate the principle into regular payments with the specified interest rate and number of years for the repayment.

To determine the cost of fuel saved, the average fuel saved per year by the solar cooling system and the real growth rate of the fuel cost have to be known first. The average annual fuel saved can be calculated using the solar fraction SF predicted by the semi-empirical equation described in Chapter V (Equation (5.13)), the total cooling load of the building L, and the seasonal energy efficiency ratio SEER of conventional chillers, as follows:

$$\text{Fuel Saved} = \frac{(SF)(L)}{SEER} \qquad\qquad (6.3)$$

The product of the solar fraction and the cooling load gives the amount of cooling load that is supplied by the solar energy source. This product divided by the seasonal energy efficiency ratio of the conventional chiller used for comparison gives the energy that otherwise has to be supplied by conventional energy sources, that is, the fuel saved.

The fuel cost at any future time can be calculated using the real growth rate of the fuel cost and the fuel cost at year zero. The fuel cost at the time m years from year zero is expressed as

$$C_{F,m} = C_{F,o} \, (1+e)^m \qquad\qquad (6.4)$$

where

$C_{F,m}$ = fuel cost at year m;

$C_{F,o}$ = fuel cost at year zero; and

e = real growth rate of fuel cost.

The real growth rate of the fuel cost is the growth rate of the fuel cost above the general economy growth rate.

The cost of fuel saved at year m is equal to the product of fuel saved and the fuel cost at that year, that is:

$$\text{Cost of Fuel Saved} = \frac{(SF)(L)}{SEER} \, C_{F,o} \, (1+e)^m \qquad\qquad (6.5)$$

It can be seen in Equation (6.5) that the cost of the fuel saved is not constant but increases with the number of years. For the annual cost analysis, however, an averaged annual cost of fuel saved is needed. To derive an averaged annual cost of fuel saved, the total cost of fuel saved during the expected system lifetime is first translated into its

present worth. The present worth of total fuel saved can be considered

as the capital already possessed. Equal annual withdrawal can be made

from this capital over the system lifetime, with the amount not yet with-

drawn earning compound interest. The average annual cost of fuel saved

is defined to be equal to the amount of this annual withdrawal. It can

be calculated by multiplying the capital recovery factor by the present

worth of the total fuel saved. The present worth of the cost of fuel

saved in year m can be written as:

$$PW_m = \frac{(SF)(L)}{SEER} \frac{C_{F,m}}{(1+i)^m} = \frac{(SF)(L)}{SEER} C_{F,o} \frac{(1+e)^m}{(1+i)^m} \tag{6.6}$$

where $(1+i)^m$ is the compound interest factor with interest rate equal

to i. Therefore, the present worth of total fuel saved is

$$PW = \frac{(SF)(L)}{SEER} C_{F,o} \sum_{m=1}^{n} (\frac{1+e}{1+i})^m \tag{6.7}$$

and the averaged annual cost of fuel saved is

$$G = [\frac{i(1+i)^n}{(1+i)^n - 1}](PW) = [\frac{i(1+i)^n}{(1+i)^n - 1}] \frac{(SF)(L)}{SEER} C_{F,o} \sum_{m=1}^{n} (\frac{1+e}{1+i})^m \tag{6.8}$$

where

    i = compound interest rate; discount rate;

    e = real growth rate of fuel cost; and

    n = number of years of system lifetime.

After the owning and operating costs and the cost of fuel saved are

all on an annual cost basis, the net annual saving can be computed. The

net annual saving is the difference between the annual cost of fuel saved

and the annual owning and operating costs as expressed by the following

equation.

$$SAV = [\frac{i(1+i)^n}{(1+i)^n - 1}] \frac{(SF)(L)}{SEER} C_{F,o} \sum_{m=1}^{n} (\frac{1+e}{1+i})^m$$

$$- [\frac{i(1+i)^n}{(1+i)^n - 1}] P - 0.01 P \tag{6.9}$$

The first term on the right is the annual cost of fuel saved defined in

Equation (6.8). The second term is the annual owning cost defined in

Equation (6.2). The third term is the annual operating cost which is

estimated to be one percent of the initial investment P.

If the net annual saving of a solar cooling system is positive, the

system is considered to be economically feasible. If the net annual

saving is negative, the system is then impractical economically. It is

important to point out that the solar fraction SF and the initial invest-

ment P are both dependent on the size of the solar cooling system. Al-

though the net annual saving is a function of many other factors, such as

the fuel cost, components cost and their lifetimes, the size of the sys-

tem can have a significant effect on the annual saving. In Figure 16

the annual saving of a solar cooling system for the base building in

Dodge City, Kansas, was plotted versus the collector area with the fuel

cost at year zero as a parameter. The annual saving is actually the sea-

sonal saving for a cooling season. The costs of the collector, storage

tank, and their associated components, i.e., C_A and C_S in Equation (6.1),

used in the calculation of the annual saving were half of the total esti-

mated costs. The reason is that these components can be used both in

solar cooling and solar heating; therefore, only half of the costs are
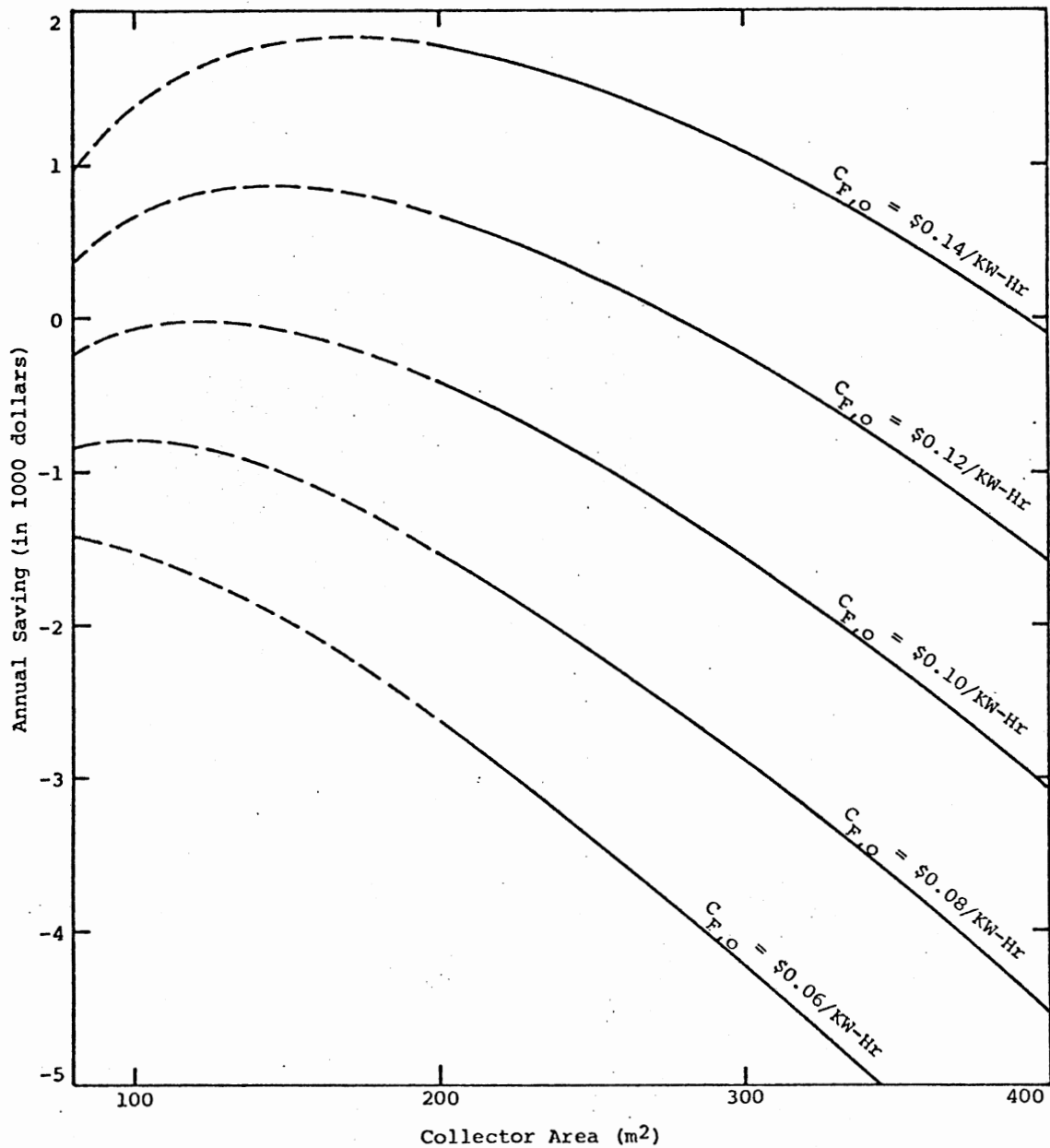
Figure 16. Annual Saving of the Solar Cooling System With
Various Collector Areas for the Base Build-
ing in Dodge City, Kansas (V_H = 20 m^3, V_C =
10 m^3, n = 20 years, e = 0.08, i = 0.08, 50%
C_A = \$200/m^2, 50% C_S = \$100/m^3, C_E = \$10,000,
SEER = 2.0)

expected to be paid by the fuel saved in cooling seasons. However, the

costs of the third category components C_E used were the full estimated

costs since these components are used for the cooling operation only.

The annual saving for the system with collector area less than 200 m^2

was plotted in the dashed line because these collector areas are outside

the range for the semi-empirical equation used to calculate the solar

fraction. The annual saving calculated in these collector area ranges

is possibly not very accurate. In any event, a collector area less than

200 m^2 is not practical for a building with 25 tons design cooling load.

It is obvious that the annual saving is a strong function of the collec-

tor area as well as the year zero fuel cost; however, the latter is not

a controllable factor. The annual saving is negative for most of the

fuel costs examined. It is also inversely proportional to the collector

area in this fuel cost range. However, the optimum collector area in-

creases with the year zero fuel cost. It can be predicted that the opti-

mum collector area will lie within the reasonable range, i.e., greater

than 200 m^2, when the fuel cost is sufficiently high. The other impor-

tant fact is that the slope of these curves decreases when the year zero

fuel cost increases; in other words, the annual saving becomes less sen-

sitive, although still significant, to the collector area. This makes

it more acceptable economically to use a larger collector area when fuel

cost is high to save more conventional fuel. In Figures 17 and 18 the

annual saving was plotted versus the chilled water storage volume and the

hot water storage volume, respectively. The annual saving is proportion-

al to both storage volumes. The effect of these two storage volumes in-

creases with the year zero fuel cost. Both of the above facts are in

the opposite of the effect of the collector area. It suggests that the

Figure 17. Annual Saving of the Solar Cooling System With Various Chilled Water Storage Volumes for the Base Building in Dodge City, Kansas ($A_C = 400$ m^2, $V_H = 20$ m^3, $n = 20$ years, $e = 0.08$, $i = 0.08$, 50% C_A = \$200/m^2, 50% C_S = \$100/m^3, C_E = \$10,000, SEER = 2.0)
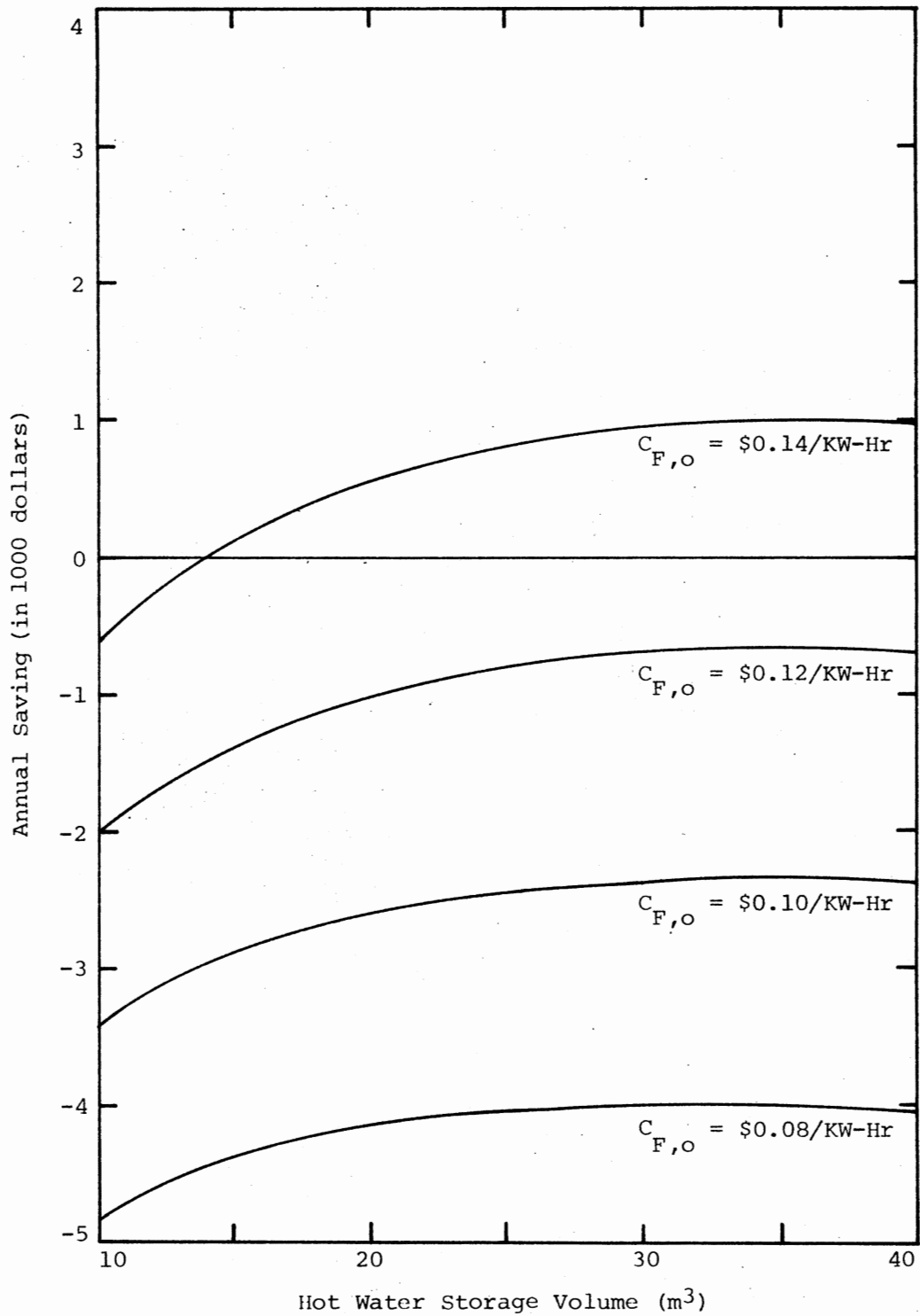
Figure 18. Annual Saving of the Solar Cooling System With
            Various Hot Water Storage Volumes for the
            Base Building in Dodge City, Kansas (A_C = 400
            m^2, V_C = 20 m^3, n = 20 years, e = 0.08, i =
            0.08, 50% C_A = $200/m^2$, 50% C_S = $100/m^3$,
            C_E = $10,000, SEER = 2.0)

proper design of these two storage volumes are more important when the
fuel cost is high. For a given year zero fuel cost, the annual saving
reaches a maximum at about 35 m^3 hot water storage volume in Figure 18,
whereas the annual cost in Figure 17 increases continuously with a possi-
ble maximum at a chilled water storage volume larger than 40 m^3. Figure
19 shows the annual saving of a system with component lifetimes equal to
25 years instead of 20 years used in the previous calculations (Figures
16, 17, and 18). The annual saving in Figure 19 compared to that in
Figure 17 is significantly greater. Therefore, improving system lifetime
should be one of the major economical concerns for solar cooling systems.

Optimization

The annual saving of a solar cooling system was shown in the previ-
ous section to be a function of the fuel cost, component costs and life-
times, discount rate, cooling load and weather conditions, and size of
system. Among these factors only the size of the system can be deter-
mined by the system designer; the other factors are determined by the
location of the system, general condition of the economy, and type of
system components available. Therefore, the problem of optimizing the
economics of a solar cooling system is a problem of finding a system size
that will yield a maximum annual saving for a given fuel cost, component
costs, component lifetimes, discount rate, location, etc.

The size of a solar cooling system is characterized by the sizes of
its collector area A_C, chilled water storage volume V_C, and hot water
storage volume V_H. Generally, there are practical limitations on the
sizes of these three components. For the solar cooling system considered
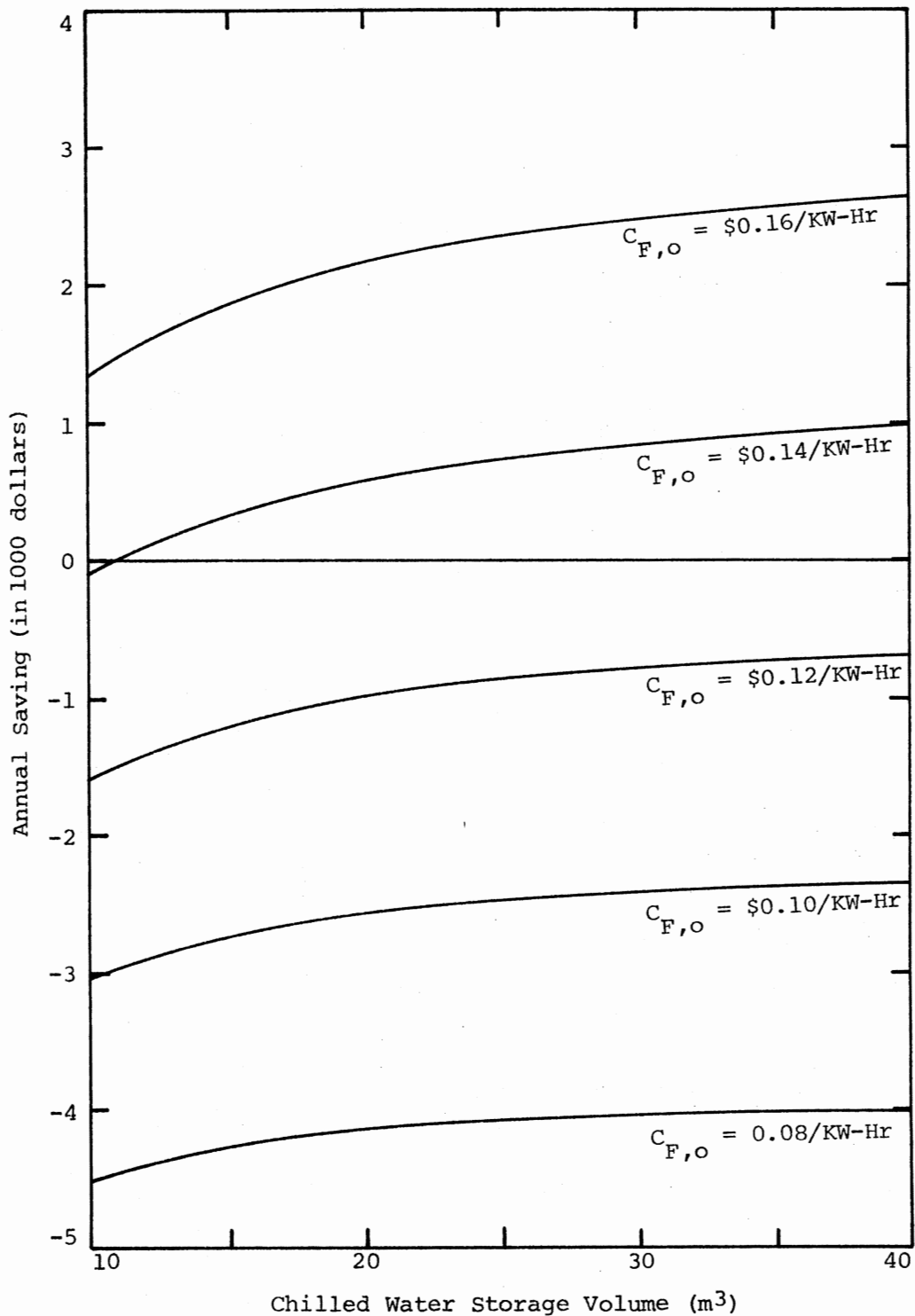in this study, the range for the collector area is between 200 m^2 and
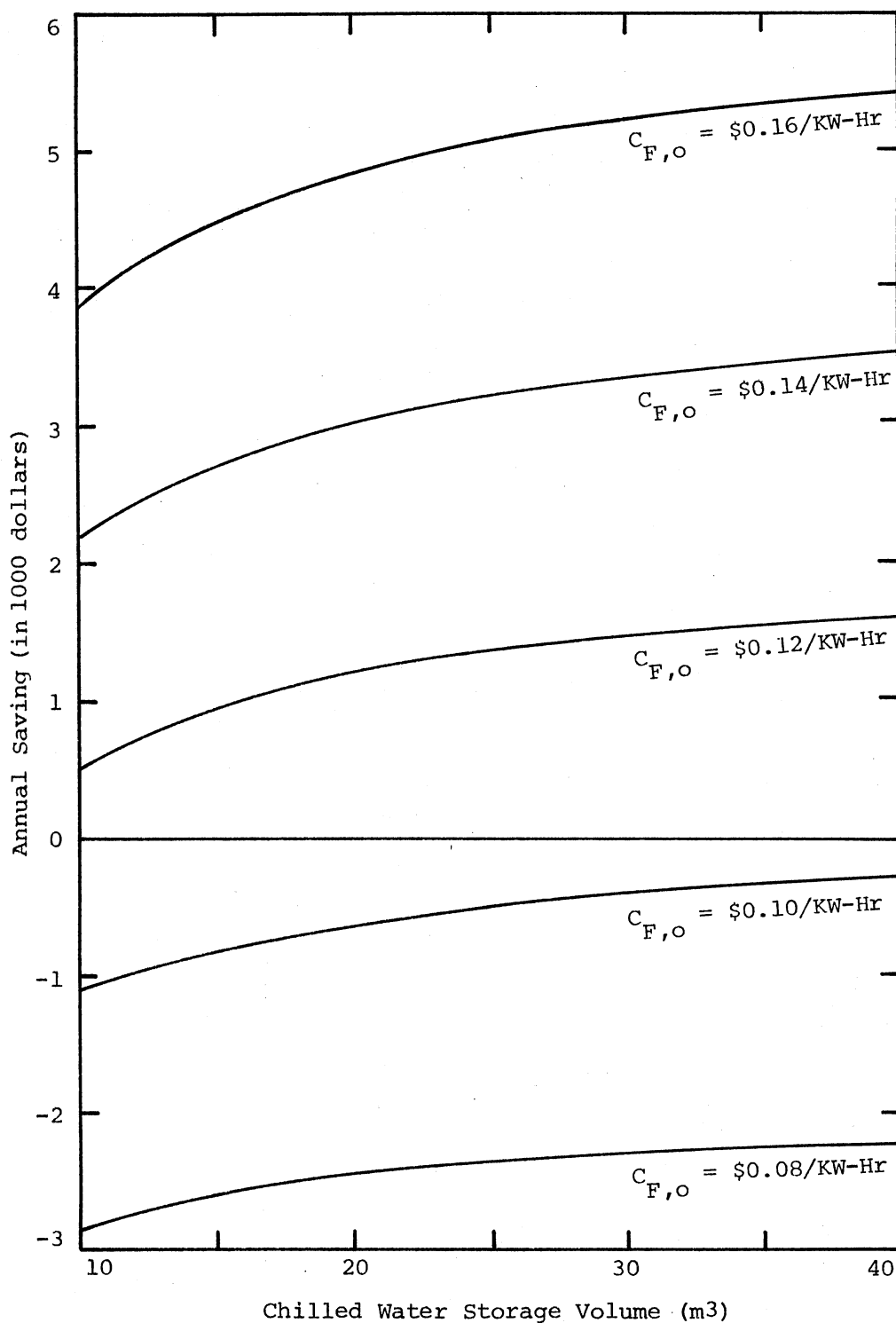
Figure 19. Annual Saving of the Solar Cooling System With
Various Chilled Water Storage Volumes for the
Base Building in Dodge City, Kansas ($A_C = 400$
$V_H = 20$ m^3, n = 25 years, e = 0.08, i = 0.08,
50% C_A = \$200/m^2, 50% C_S = \$100/m^3, C_E =
\$10,000, SEER = 2.0)

$400 \ m^2$, and for both storage volumes is between $10 \ m^3$ and $40 \ m^3$. The

sizes of these three components within their respective ranges which

yields the maximum annual saving are the optimum sizes desired. In

other words, the maximum of Equation (6.9) is sought under the following

inequality constraints:

$$200 \ m^2 \leq A_C \leq 400 \ m^2 \tag{6.10}$$

$$10 \ m^3 \leq V_H \leq 40 \ m^3 \tag{6.11}$$

$$10 \ m^3 \leq V_C \leq 40 \ m^3 \tag{6.12}$$

Because of the presence of the inequality constraints, the problem can-

not be solved analytically. Instead, a numerical search method is

required.

There are several search methods available for finding the maximum

of a multivariable, nonlinear function subject to inequality constraints

(55). The method used in this study is a procedure developed by Fiacco

and McCormick (56). The technique uses the original objective function

and the problem constraints to form a new objective function which can

be maximized by unconstrained, multivariable search method such as the

generalized Newton-Raphson method. The computer program listings of

this procedure can be found in Kuster and Mize's Optimization Technique

With FORTRAN (55).

The optimum annual saving and component sizes for the system in

Dodge City, Kansas were plotted versus the year zero fuel cost in Figures

20 and 21, respectively. The component costs and lifetimes used in these

two figures were estimated based on the data found in the ERDA Facilities

Solar Design Handbook (53).
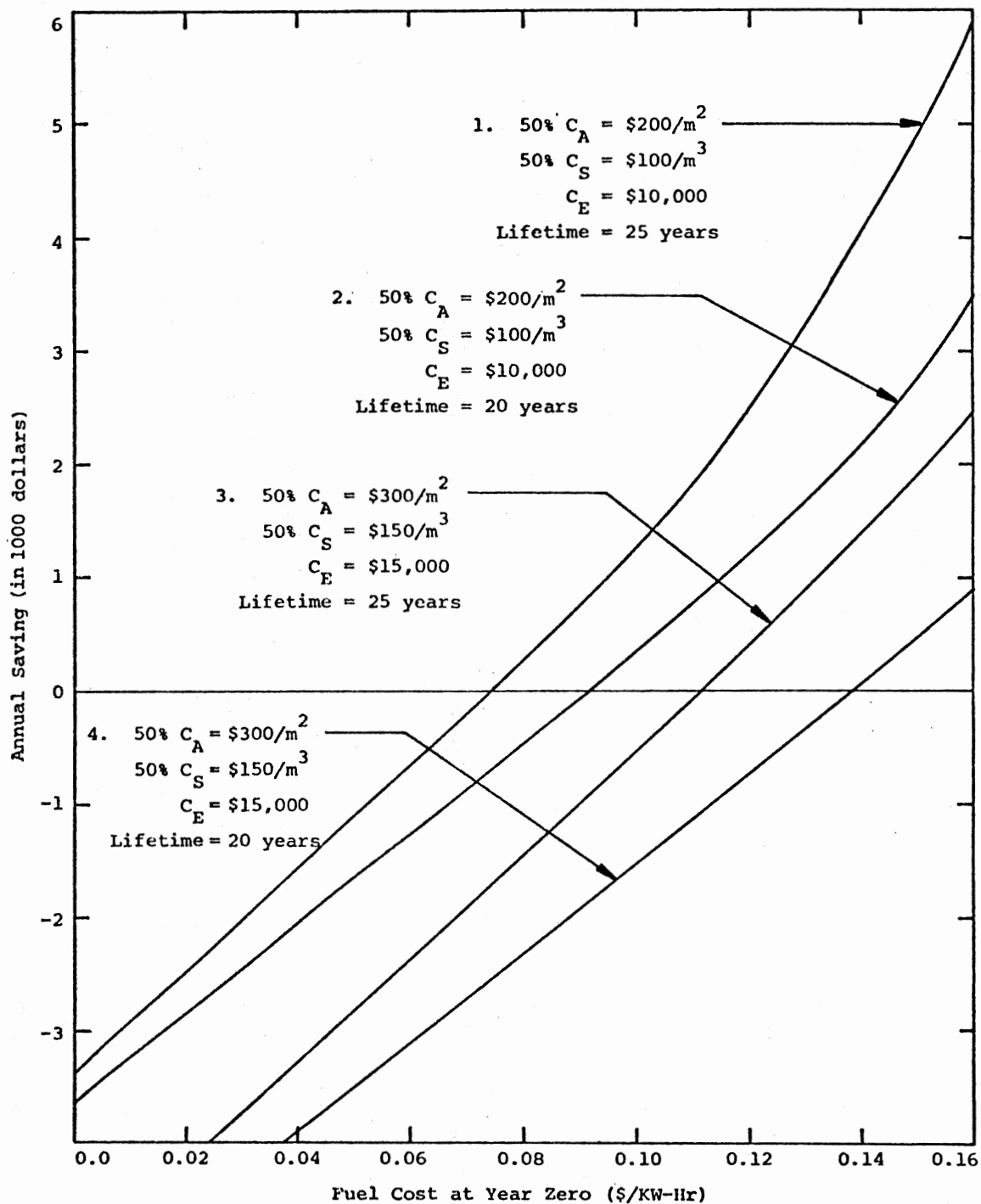
Figure 20. Optimum Annual Saving of the Solar Cooling System
for the Base Building in Dodge City, Kansas,
Versus Year Zero Fuel Cost (e = 0.08, i = 0.08,
SEER = 2.0)
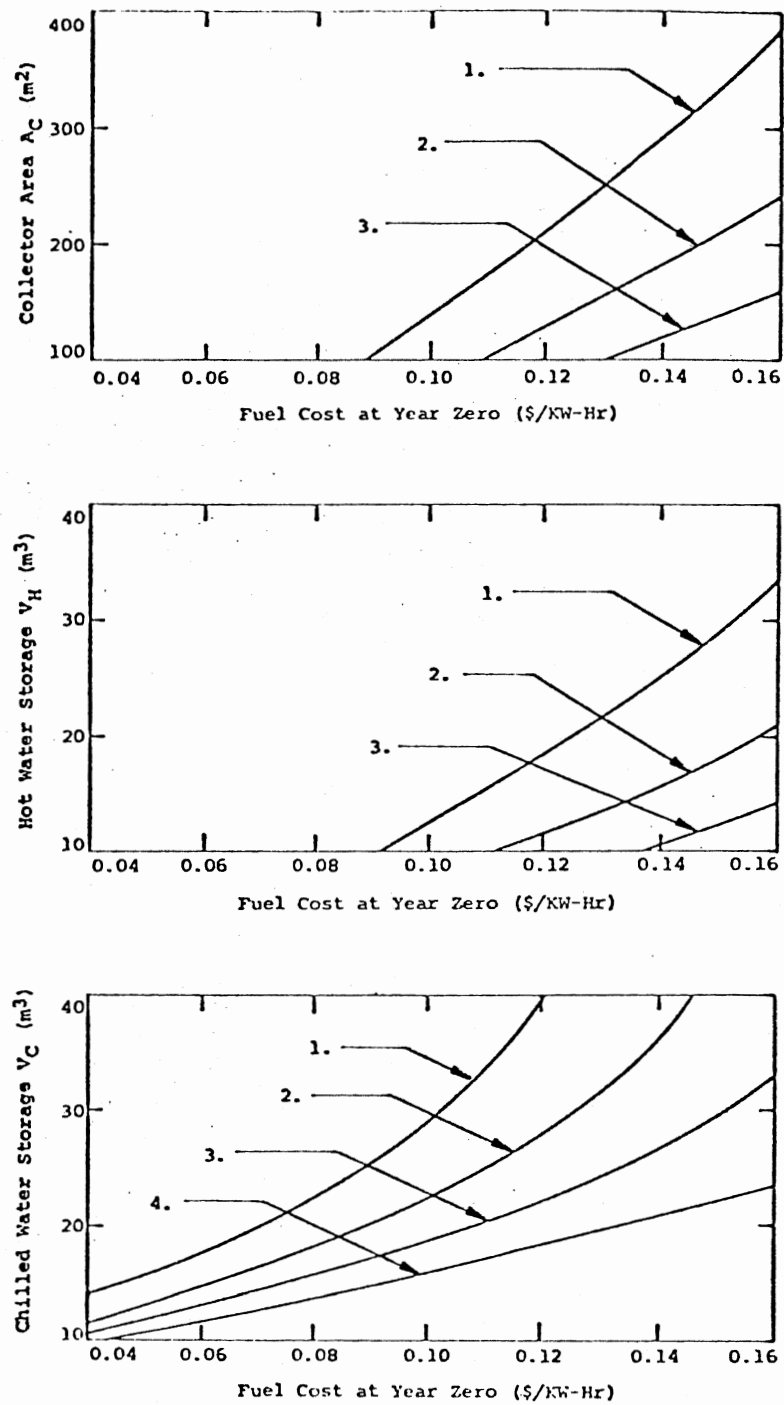
Figure 21. Optimum Sizes of A_C, V_H, and V_C of the Solar Cooling System. (The curves are numbered in the same fashion as in Figure 20.)

The four classes shown were to provide a general range of possible component costs and lifetimes. However, these should only be used as references, since the actual component costs and lifetimes vary with location and are also time-dependent. The optimum saving is a strong function of the fuel cost as expected. The effect of component cost on the annual saving is a weak function of the fuel cost; this can be seen in Figure 20 as curves 1 and 3 and curves 2 and 4 are almost parallel. The effect of component lifetime, on the other hand, is smaller when fuel cost is high, i.e., curves 1 and 2 and curves 3 and 4 diverge when fuel cost increases. It seems that increasing component lifetime at the expense of higher cost is not practical when fuel cost is low, but becomes favorable when fuel cost is sufficiently high. The optimum size of chilled water storage volume is always greater than the optimum size of the hot water storage volume for any given year zero fuel cost. The optimum collector areas are small because of high collector cost. The close relationship between the hot water storage volume and the collector area can also be seen in Figure 21. This may be the reason for the optimum hot water storage volume being smaller than the optimum chilled water storage volume because hot water storage volume has to be reduced to fit the small collector area while chilled water storage volume does not. It needs to be pointed out here that in Figure 21, when the optimum size of any of the three components is not within its respective ranges considered, the size used is the upper or lower bound value, depending on whether it is above or below the range.

CHAPTER VII

CONCLUSIONS AND RECOMMENDATIONS

Conclusions

The findings of this study were classified into three categories. In the first category are the findings concerning the effect of the size of the solar cooling system on its performance, specifically the effect of the sizes of the chilled water storage volume, the hot water storage volume, and the collector area. In the second category are the findings concerning the semi-empirical equation for predicting the solar cooling system performance. In the third category are those relating to the solar cooling system economics.

Size of the Solar Cooling System

1. The use of chilled water storage in conjunction with hot water storage is an effective scheme for reducing the disadvantageous effects of inefficiency of the absorption chiller due to the start-up transient and the time difference between the peak cooling load and the peak solar radiation. The effectiveness of this scheme depends largely on the proper sizing of the chilled water storage, hot water storage, and collector area with respect to the cooling load and available solar radiation.

2. The long-term COP of the absorption chiller is higher when the

ratio of the total solar energy collected to the total cooling load is lower. However, the solar fraction of the solar cooling system is lower in these despite the higher chiller COP because of the lack of available solar energy (see Figures 8 through 11).

3. The long-term COP of the absorption chiller and the solar fraction of the solar cooling system is more sensitive to the sizes of chilled water storage and hot water storage when the ratio of the total solar energy collected to the total cooling load is higher (see Figures 8 through 11). Therefore, the proper design of the sizes of chilled water storage and hot water storage is more important in locations where the solar radiation is more abundant.

4. Generally speaking, increasing the chilled water storage volume improves the long-term COP of the absorption chiller. The solar fraction of the system will also be improved, largely due to the higher chiller COP. However, there exists a maximum chilled water storage volume above which further increase of the volume effects little improvement of the system performance. This maximum chilled water storage volume is a function of the total cooling load, the total solar energy collected, and the hot water storage volume. For the system considered in this study, the maximum chilled water storage volume appeared to be about 40 m^3. The major improvement of the system performance was realized in the first 20 m^3 increment of the chilled water storage volume, i.e., from 0 m^3 to 20 m^3. The improvement resulting from the second 20 m^3 increment, from 20 m^3 to 40 m^3, was only about one-eighth of the first improvement (see Figures 8 and 9).

5. A large hot water storage volume is generally favorable for the system performance. However, larger hot water storage volume does not

significantly improve the long-term COP of the absorption chiller. The improvement of the solar fraction is mostly due to higher collector efficiency. There is also a maximum hot water storage volume above which the system performance cannot be improved by further increasing the hot water storage volume. This maximum hot water storage volume is a strong function of the collector area. For the system considered in this study the maximum hot water storage volume is about 40 m^3 when the collector area equals 400 m^2. The improvement of solar fraction from 10 m^3 to 20 m^3 hot water storage volume was most visible while the improvement from 30 m^3 to 40 m^2 became significantly small (see Figures 10 and 11).

6. The long-term COP of the absorption chiller decreases when the collector area increases (see Figure 12). As a result, the contribution of the additional collector area to the solar fraction becomes smaller as the total collector area becomes larger.

7. The increasing collector area has the same effect on the long-term COP of the absorption chiller as decreasing the hot water storage volume (see the COP curves in Figures 10 and 12). By properly balancing the increase of collector area with the increase of hot water storage volume, the decrease of the chiller COP due to larger collector area can be minimized.

Semi-Empirical Equation

1. The long-term averaged seasonal solar fraction of a solar cooling system can be expressed in terms of four dimensionless parameters, V_H^*, V_C^*, T^*, and A_C^* (Equation (5.13)). The predictions of the semi-empirical equations were found to be within six percent of the simulation results

for seven SOLMET stations which have typical meteorological year data

(see Figures 14 and 15).

2. The semi-empirical equation was found to be valid for locations with considerable differences in their weather patterns. This is because the effect of different weather conditions was implicitly considered when forming the four dimensionless parameters, i.e., the parameters were non-dimensionalized with weather dependent factors such as the total solar radiation, the total cooling load, etc.

3. The use of the semi-empirical equation is limited for systems with collector area between 240 m^2 and 440 m^2, and chilled water storage volume and hot water storage volume between 10 m^3 and 40 m^3. The fact that the equation was developed from the simulation results of a system with a 25-ton absorption chiller and double-glazed selective-surface solar energy collectors also restricts the validity of this equation to solar cooling systems of similar design.

Solar Cooling System Economics

1. The averaged annual saving of a solar cooling system is a function of the fuel cost, component costs, component lifetime, discount rate, cooling load, weather conditions, and system size. Among these factors, the discount rate is assumed to be a constant. The cooling load and the typical weather condition are fixed for a given location. The fuel cost and its growth rate are constants in a given year for a given location. The variations of the component costs and lifetimes are limited. Only the system size can be easily controlled by system designers to maximize the annual saving.

2. For the solar cooling system considered in this study, the optimum collector area is smaller than 200 m^2 when the fuel cost is lower than $0.14 per KW-HR. The annual saving of the system is inversely proportional to the collector area in this range of year zero fuel cost for the desirable collector area range between 200 m^2 and 400 m^2. Only after the year zero fuel cost becomes substantially larger than $0.14 per KW-HR, can the optimum collector area be expected to be within the desirable collector area range (see Figure 16). The optimum chilled water storage volume is generally within the desirable range, i.e., between 10 m^3 and 40 m^3. The optimum hot water storage volume is largely related to the collector area. Because the optimum collector area is small when the fuel cost is low, the optimum hot water storage volume is also small in this circumstance. The sensitivities of the annual saving with respect to the chilled water storage and hot water storage increase with the fuel cost, whereas the sensitivity of the annual saving with respect to the collector area decreases when fuel cost increases.

3. The effect of system lifetime on the annual saving is significantly large. When the fuel cost is high, increasing the system lifetime is generally favorable even if it means some increase in component costs. However, when the fuel cost is low, most of the extra savings due to the longer system lifetime may be offset by the increase of component costs.

4. The annual saving is a strong function of fuel cost. For the system considered in this study, the annual saving is negative when the year zero fuel cost is below $0.10 per KW-HR. The fuel cost has to be higher than $0.14 per KW-HR for most systems to realize positive annual savings.

Recommendations

The recommendations for future study are outlined as follows:

1. The present study concentrated on the performance of the solar system in the cooling mode. Future study should include the performance of the same system in the heating mode. During heating operations the chilled water storage tank can be used to store hot water. It is also possible to use the absorption chiller as a heat pump, to improve its load factor, and to improve its investment return. A complete analysis of the performance of the solar system in both cooling and heating modes is needed to provide a better assessment of the system.

2. The semi-empirical equation derived in this study may be extended to accommodate a greater variation of collector types. This may be accomplished by redefining A_C^* and V_H^* to take into consideration the effect of various collector characteristics. It is also desirable to consider different types of absorption chillers. However, to consider the effect of different types of absorption chillers may require the introduction of new parameters, since the existing parameters do not seem to have this capacity.

3. The predictions of the semi-empirical equation have been compared satisfactorily with simulation results of the system at seven locations. To further confirm the validity of this equation, its predictions should be compared with simulation results of the system at as many other locations as possible. If necessary, the simulation results at other locations may be used to modify the coefficients of the semi-empirical equation to improve the accuracy of its predictions.

4. Performance data of the solar cooling system with chilled water storage are needed to evaluate the simulation model and the semi-

empirical equation. Since the semi-empirical equation is derived for long-term system performance predictions, several years of performance data are required for evaluating the equation.

BIBLIOGRAPHY

(1) Eisenstadt, M. M., F. M. Flanigan, and E. A. Farber. "Solar Air Conditioning With Ammonia-Water Absorption Refrigeration System." ASME, Paper No. 59-A-276, December, 1959.

(2) Chung, R., J. A. Duffie, and G. O. G. Lof. "A Study of a Solar Air Conditioner." Mech. Engng., Vol. 85, No. 8 (August, 1963), pp. 31-35.

(3) Farber, E. A., F. M. Flanigan, L. Lopez, and R. W. Polifka. "Operation and Performance of the University of Florida Solar Air-Conditioning System." Solar Energy, Vol. 10, No. 2 (1966), pp. 91-95.

(4) Sheridan, N. R. "Performance of the Brisbane Solar House." Solar Energy, Vol. 13, No. 4 (July, 1972), pp. 395-401.

(5) Ingley, H. A. "Design and Development of a Solar Powered Ammonia/Water Air Conditioning System." Build. Syst. Des., Vol. 72, No. 4 (June-July, 1975), pp. 14-16.

(6) Charters, W. W. S., and L. F. Peterson. "Free Convection Suppression Using Honeycomb Cellular Materials." Solar Energy, Vol. 13, No. 4 (July, 1972), pp. 353-361.

(7) Pellette, P., M. Cobble, and P. Smith. "Honeycomb Thermal Trap." Solar Energy, Vol. 12, No. 2 (1968), pp. 263-265.

(8) Eaton, C. B., and H. A. Blum. "The Use of Moderate Vacuum Environments as a Means of Increasing the Collection Efficiencies and Operating Temperature of Flat-Plate Solar Collectors." Solar Energy, Vol. 17, No. 3 (1975), pp. 151-158.

(9) Minardi, J. E., and H. N. Chuang. "Performance of a Black Liquid Flat-Plate Solar Collector." Solar Energy, Vol. 17, No. 3 (1975), pp. 179-183.

(10) Hottel, H. C., and T. A. Unger. "The Properties of a Copper Oxide-Aluminium Selective Black Surface Absorber of Solar Energy." Solar Energy, Vol. 3, No. 3 (1959), pp. 10-15.

(11) Silo, R. S., and P. A. Mladinic. "Solar Heater Using Selective Surfaces." Applied Solar Energy, Vol. 5, No. 5 (1969), pp. 18-23.

(12) Kudryashova, M. D. "New Selective Coatings for Collector Surfaces of Solar Plants." Applied Solar Energy, Vol. 5, No. 4 (1969), pp. 82-88.

(13) Peterson, R. E., and J. W. Ramsey. "Thin Film Coatings in Solar-Thermal Power Systems." J. Vac. Sci. Technol., Vol. 12, No. 1 (1975), pp. 174-181.

(14) McDonald, G. E. "Spectral Reflectance Properties of Black Chrome for Use as a Solar Selective Coating." Solar Energy, Vol. 17, No. 2 (1975), pp. 119-122.

(15) Driver, P. M., R. W. Jones, C. L. Riddiford, and R. J. Simpon. "A New Chrome Black Selective Absorbing Surface." Solar Energy, Vol. 19, No. 3 (1977), pp. 301-306.

(16) Lushiku, E. M., and K. R. O'Shea. "Ellipsometry in the Study of Selective Radiation-Absorbing Surface." Solar Energy, Vol. 19, No. 3 (1977), pp. 271-276.

(17) Blickensderfer, R., D. K. Deardorff, and R. L. Lincoln. "Spectral Reflectance of TiNx and ZrNx Films as Selective Solar Absorbers." Solar Energy, Vol. 19, No. 4 (1977), pp. 429-432.

(18) Goodman, R. D., and A. G. Menke. "Effect of Cover Plate Treatment on Efficiency of Solar Collectors." Solar Energy, Vol. 17, No. 4 (1975), pp. 207-211.

(19) Stoecker, W. F., and L. D. Reed. "Effect of Operating Temperature on the Coefficient of Performance of Aqua-Ammonia Refrigeration Systems." ASHRAE Transactions, Vol. 77, Part I (1971), p. 163.

(20) Whitlow, E. D. "Relationship Between Heat Source Temperature, Heat Sink Temperature and Coefficient of Performance for Solar-Powered Absorption Air Conditioner." ASHRAE Transactions, Vol. 82, Part I (1976), pp. 950-958.

(21) Porter, J. M. "The Use of Commercially Available Absorption Units on Solar-Powered Cooling Systems." ASHRAE Transactions, Vol. 82, Part I (1976), pp. 943-949.

(22) Sargent, S. L., and W. A. Beckman. "Theoretical Performance of an Ammonia-Sodium Thiocyanate Intermittent Absorption Refrigeration Cycle." Solar Energy, Vol. 12, No. 2 (1968), pp. 137-146.

(23) Swartman, R. K., V. Ha, and C. Swaminathan. "Comparison of Ammonia-Water and Ammonia-Sodium Thiocyanate as the Refrigerant-Absorbent in a Solar Refrigeration System." Solar Energy, Vol. 17, No. 2 (1975), pp. 123-127.

(24) Farber, E. A., C. A. Morrison, and H. A. Ingley. "Selection and Evaluation of the University of Florida's Solar Powered Absorption Air Conditioning System." ASME, Paper No. N-74-WA/Sol-6 (for meeting, November 17-22, 1974).

(25) Ellington, R. L. "The Absorption Cooling Process." Institute of Gas Technology, Research Bulletin No. 14, Chicago, Illinois, 1957.

(26) Macriss, R. A. "Selecting Refrigerant-Absorbent Fluid Systems for Solar Energy Utilization." ASHRAE Transactions, Vol. 82, Part I (1976), pp. 975-988.

(27) Chinnapa, J. C. V. "Solar Operation of Ammonia-Water Multistage Air Conditioning Cycles in the Tropic." Solar Energy, Vol. 16, Nos. 3-4 (December, 1974), pp. 165-170.

(28) Phillips, B. A. "Absorption Cycles for Air-Cooled Solar Air Conditioning." ASHRAE Transactions, Vol. 82, Part I (1976), pp. 966-974.

(29) Wilbur, P. J., and C. E. Mitchell. "Solar Absorption Air Conditioning Alternatives." Solar Energy, Vol. 17, No. 3 (1973), pp. 193-199.

(30) Wilbur, P. J., and J. R. Mancini. "A Comparison of Solar Absorption Air Conditioning Systems." Solar Energy, Vol. 18, No. 6 (1976), pp. 569-576.

(31) Anderson, P. P. "Solar-Operated Absorption Water Chiller--A comparison of Aqueous Bromide and Aquea Ammonia Cycles." ASHRAE Transactions, Vol. 82, Part I (1976), pp. 959-965.

(32) Picking, J. W., Jr. Personal communication. ARKLA Industries, Inc., Evansville, Indiana, September, 1978.

(33) Ward, D. S., T. A. Weiss, and G. O. G. Lof. "Preliminary Performance of CSU Solar House I Heating and Cooling System." Solar Energy, Vol. 18, No. 6 (1976), pp. 541-548.

(34) Ishibashi, T. "The Result of Cooling Operation of Yazaki Experimental Solar House One." Solar Energy, Vol. 21, No. 1 (1978), pp. 11-16.

(35) Beckman, W. A. "Ingenuity and Experiment Are Needed to Advance Solar Cooling." Sunworld, No. 6 (November, 1977), pp. 2-6.

(36) Rauch, J. S., and B. D. Wood. "Steady State and Transient Performance Limitations of the ARKLA Solaire Absorption Cooling System." Sharing the Sun; Sol. Tech. in the Seventies, Vol. 3 (1976), pp. 387-405.

(37) Miller, D. K. "The Performance of Water Cooled Lithium Bromide Absorption Units for Solar Energy Applications." Heating, Piping and Air Conditioning (January, 1976), pp. 45-51.

(38) Newton, A. B. "Optimizing Solar Cooling Systems." ASHRAE J. (November, 1976), pp. 26-31.

(39) Ward, D. S., G. O. G. Lof, and T. Uesaki. "Cooling Subsystem Design in CSU Solar House III." Solar Energy, Vol. 20, No. 2 (1978), pp. 119-126.

(40) Hottel, H. C., and A. Whillier. "Evaluation of Flat Plate Solar Collector Performance." Trans. of the Conference on the Use of Solar Energy, Vol. 2, Part I, University of Arizona Press (1958), pp. 74-104.

(41) Duffie, J. A., and W. A. Beckman. Solar Energy Thermal Processes, (Chapter 7). New York: John Wiley & Sons, 1974.

(42) ASHRAE Handbook of Fundamentals (Chapter 1). New York: American Society of Heating, Refrigerating and Air Conditioning Engineers, Inc., 1977, pp. 1.18-1.24.

(43) TRNSYS: A Transient Simulation Program. Prepared by the Solar Energy Laboratory, University of Wisconsin-Madison, Madison, Wisconsin, October, 1977.

(44) Hall, I. J. et al. "Generation of Typical Meteorological Years for 26 Solmet Stations." ASHRAE Transactions, Vol. 85, Part 2 (to be published 1979).

(45) Freeman, T. L. "Investigation of the Solmet Typical Meteorological Year." Paper presented to the 1979 International Congress, International Solar Energy Society, Atlanta, Georgia, May 28-June 1, 1979.

(46) Stoecker, W. F. Procedures for Simulating the Performance of Components and Systems for Energy Calculation. 3rd ed. New York: American Society of Heating, Refrigerating and Air-Conditioning Engineers, Inc., 1975.

(47) ASHRAE Handbook of Fundamentals (Chapter 25). New York: American Society of Heating, Refrigerating and Air-Conditioning Engineers, Inc., 1977, pp. 25.37-25.39.

(48) McQuiston, F. C., and J. D. Parker. Heating, Ventilating, and Air Conditioning: Analysis and Design (Chapter 8). New York: John Wiley & Sons, 1977, pp. 253-257.

(49) ASHRAE Handbook of Fundamentals (Chapter 23). New York: American Society of Heating, Refrigerating and Air-Conditioning Engineers, Inc., 1977, pp. 23.3-23.22.

(50) Schenck, H., Jr. Theories of Engineering Experimentation (Chapter 6). St. Louis: McGraw-Hill Book Company, 1968.

(51) Stoecker, W. F. Design of Thermal Systems (Chapter 5). St. Louis: McGraw-Hill Book Company, 1971.

(52) Chandler, J. P., and L. W. Jackson. Personal communication. Department of Computing and Information Science, Oklahoma State University, Stillwater, Oklahoma, 1978.

(53) ERDA Facilities Solar Design Handbook. U.S. Energy Research and Development Administration. Prepared by the University of California, Los Alamos Scientific Laboratory, Los Alamos, New Mexico, 1977.

(54) Stoecker, W. F. Design of Thermal Systems (Chapter 3). St. Louis: McGraw-Hill Book Company, 1971.

(55) Kuster, J. L., and J. H. Mize. Optimization Techniques With FORTRAN (Chapter 10, Section IV). St. Louis: McGraw-Hill Book Company, 1973, pp. 412-463.

APPENDIX A

DESCRIPTION OF THE BASE BUILDING AND

ITS COOLING LOAD CALCULATION

The base building used for calculating the cooling load has the following physical parameters:

South wall: 4.27 m high and 92.6 m wide

East wall: 7.32 m wide

West wall: 7.32 m wide

North wall: 3.66 m high and 92.6 m wide.

There are 15 windows, each measures 1.02 m by 1.02 m, as well as a 31.76 m^2 door area in the north wall. There is no window or door in the other three walls. The walls and ceiling are insulated with six inches of fiber glass insulation materials.

The lighting load in the building was assumed to be 72 KJ/Hr-m^2 from 8:00 a.m. to 5:00 p.m. and no lighting load from 5:00 p.m. to 8:00 a.m. during the week. The lighting load was reduced to 36 KJ/Hr-m^2 on Saturday and 18 KJ/Hr-m^2 on Sunday. The building was assumed to be occupied by 60 persons from 8:00 a.m. to 5:00 p.m. during the week, by 30 persons on Saturday, and by 15 persons on Sunday. From 5:00 p.m. to 8:00 a.m. the next day, the building was assumed to be unoccupied.

The input to the TRNSYS program for calculating the cooling load of this building is listed in the following program listing.

```
            SUBROUTINE TYPE22 (TIME,XIN,OUT,T,DTDT,PAR,INFO)
C
C     LATENT COOLING LOAD FROM OUTDOOR AIR AND PEOPLE
C
C     XIN(1)--WET BULB TEMPERATURE, DEGREE C
C     XIN(2)--DRY BULB TEMPERATURE, DEGREE C
C     XIN(3)--TIME DEPENDENT PEOPLE LOAD-SENSIBLE
C
C     PAR(1)--VOLUME OF BUILDING
C     PAR(2)--AIR CHANGES PER HOUR
C     PAR(3)--HOUR SUMMER BEGINS
C     PAR(4)--HOUR SUMMER ENDS
C     PAR(5)--NUMBER OF PEOPLE IN BUILDING
C
C     OUT(1)--LATENT COOLING LOAD FROM OUTDOOR AIR, KJ/HR
C     OUT(2)--LATENT COOLING LOAD FROM PEOPLE, KJ/HR
C     OUT(3)--TOTAL LATENT COOLING LOAD
C
      DIMENSION XIN(3),OUT(3),PAR(5),INFO(8)
      INFO(6)=3
      IF (TIME.LT.PAR(3).OR.TIME.GT.PAR(4)) GO TO 10
      TWBK=XIN(1)+273.16
      TDBK=XIN(2)+273.16
C
C       CALCULATE VAPOR PRESSURE OF OUTSIDE AIR
      X=647.27-TWBK
      Y=3.2438+(5.683E-3+1.17024E-8*X*X)*X
      Y=Y*X/(TWBK*(1.0+2.18785E-3*X))
      P=1.65807E5/(10.0**Y)
C
C       LATENT HEAT PER CUBIC METER OF AIR EXCHANGED
C                   IN KJ/M**3
      HEAT=(706.0*P/TDBK)-22.984
C
C       LATENT HEAT PER HOUR
      HEAT=HEAT*PAR(1)*PAR(2)
      IF (HEAT.LT.0.0) HEAT=0.0
C
C       LATENT HEAT FROM PEOPLE
      HEAPLP=PAR(5)*189.6
      IF (XIN(3).LE.0.0) HEAPLP=0.0
C
C       TOTAL LATENT LOAD
      TLALO=HEAT+HEAPLP
      OUT(1)=HEAT
      OUT(2)=HEAPLP
      OUT(3)=TLALO
      RETURN
10    OUT(1)=0.0
      OUT(2)=0.0
      OUT(3)=0.0
      RETURN
      END
```

```
***
***    SAMPLE INPUT
***

    SIMULATION 0,  4416,  1

    UNIT 1   TYPE 9   DATA READER
        PARAMETERS 4
        4,  1,  9,  1
(F5.1,F7.1,2F5.1)

    UNIT 2 TYPE 16   RADIATION PROCESSOR
        PARAMETERS 14
        1,    121,   36.1,   4871,   0.2,   0.0,   90,   0.0,   90,
        90,   90,   180,   90,   270
        INPUTS 1
        1,2
        0.0

    UNIT 3 TYPE 17   EAST WALL
        PARAMETERS 17
        1, 0.5, 0.8, 4, 2,  58,   0,   1,   0,   1,   1,   0.00928,
        0.0287,   0.0036,   0.142E-4,   -0.1245,   0.162E-3
        INPUTS 4
        1,1   2,8   1,4   12,2
        20,   0,   0,   20

    UNIT 4 TYPE 17   WEST WALL
        PARAMETERS 17
        1, 0.5, 0.8, 4, 2, 58,   0,   1,   0,   1,   1,   0.928E-2,
        0.287E-1,   0.36E-2,   0.142E-4,  -0.1245,   0.162E-3
        INPUTS' 4
        1,1   2,10   1,4   12,2
        20,     0,   0,   20

    UNIT 5 TYPE 17   SOUTH WALL
        PARAMETERS 17
        1, 0.5, 0.8, 4, 2, 394.9, 0, 1, 0, 1, 1, 0.928E-2,
        0.287E-1,   0.36E-2,   0.142E-4,   -0.1245,   0.162E-3
        INPUTS 4
        1,1   2,1   1,4   12,2
        20,   0,   0,   20

    UNIT 6 TYPE 17   NORTH WALL
        PARAMETERS 17
        1, 0.5, 0.8, 4, 2, 338.5, 0.9, 1, 0.055,   0.5,   1,
        0.928E-2, 0.287E-1, 0.364E-2, 0.142E-4,  -0.1245,
        0.621E-3
        INPUTS 4
        1,1   2,9   1,4   12,2
        20,   0,   0,   20

    UNIT 7 TYPE 17  ROOF
        PARAMETERS 19
```

```
        1,  0.8,  0.9,  5,  3,  677,  0,  1,  0,  1,  -1,
        0.855E-3,  0.125E-1,  0.1E-1,  0.815E-3,  0.376E-5,
        -0.4742,  0.06,  -0.175E-2
        INPUTS 4
        1,1  2,4  1,4  12,2
        20,  0,  0,  20
```

     UNIT 8 TYPE 14   TIME DEPENDENT LIGHTING LOAD
***
***   ASSUME 20 W/M*M OR 72 KJ/HR-M*M
***   FLLOR AREA 677 M*M, WEIGHTING FACTOR = 0.8
***   TOTAL LOAD (72)(677)(0.8) = 39000 KJ/HR
***   HALF LOAD ON SATURDAY, QUARTER LOAD ON SUNDAY
***

```
        PARAMETERS 60
        0,0  7.5,0   8.5,39000  16.5,39000  17.5,0  31.5,0
        32.5,39000  40.5,39000  41.5,0  55.5,0  56.5,39000
        64.5,39000  65.5,0  79.5,0  80.5,39000
        88.5,39000  89.5,0  103.5,0  104.5,39000
        112.5,39000  113.5,0  127.5,0  128.5,19500
        136.5,19500  137.5,0  151.5,0  152.5,9750
        160.5,9750  161.5,0  168,0
```

     UNIT 9 TYPE 14   TIME DEPENDENT SENSIBLE PEOPLE LOAD
***
***   ASSUME 73 W/PERSON OR 263 KJ/HR-PERSON SENSIBLE LOAD
***   60 PERSONS OCCUPANCY,   WEIGHTING FACTOR = 0.8
***   TOTAL SENSIBLE LOAD 263*0.8*60 = 12600 KJ/HR
***   HALF LOAD ON SATURDAY, QUARTER LOAD ON SUNDAY
***

```
        PARAMETERS 60
        0,0  7.5,0  8.5,12600  16.5,12600  17.5,0  31.5,0
        32.5,12600  40.5,12600  41.5,0  55.5,0  56.5,12600
        64.5,12600  65.5,0  79.5,0  80.5,12600
        88.5,12600  89.5,0  103.5,0  104.5,12600
        112.5,12600  113.5,0  127.5,0  128.5,6300  136.5,6300
        137.5,0  151.5,0  152.5,3150,  160.5,3150  161.5,0
        168,0
```

     UNIT 10 TYPE 22   LATENT COOLING LOAD
```
        PARAMETERS 5
        2683,  0.186,  0,  4416,  60
        INPUTS 3
        1,3  1,1  9,1
        0.0,  0.0,  0.0
```

     UNIT 11 TYPE 15   SUMS CONDUCTION TERMS
```
        PARAMETERS 11
        0,  0,  3,  0,  3,  0,  3,  0,  3,  0,  3
        INPUTS 5
        3,2  4,2  5,2  6,2  7,2
        10,  10,  10,  10,  10
```

```
UNIT 12 TYPE 19   LOAD CALCULATION
   PARAMETERS 17
   1,  2683,  0.25,  677,  1,  5.0E3,  2.0E3,  -1,  0,
   214.5,  5,  0,  0,  20,  25,  20,  0
   INPUTS 5
   1,1  11,1  6,3  8,1  9,1
   20,  0,  0,  0,  0

UNIT 13  TYPE 15  SUMS SENSIBLE LOAD AND LATENT LOAD
   PARAMETERS 3
   0,  0,  3
   INPUTS 2
   12,1  10,3
   10,  10

UNIT 21 TYPE 25  WRITE DISC LU--10
   PARAMETERS 4
   1,  0,  4416,  10
   INPUTS 1
   13,1
   TOTLO

END
```

APPENDIX B

SUBROUTINE AND SAMPLE INPUT FOR THE TRNSYS PROGRAM

USED FOR THE SOLAR COOLING SYSTEM SIMULATION

```
      SUBROUTINE TYPE29 (TIME,XIN,OUT,T,DTDT,PAR,INFO)
C
C     RECIPROCATING CHILLER
C
C     XIN(1)---CHILLED WATER INLET TEMP., DEGREE C
C     XIN(2)---CHILLED WATER FLOWRATE, KG/HR
C     XIN(3)---CONTROL SIGNAL, =1 CHILLER IS TURNED ON, =0 OFF
C
C     OUT(1)---CHILLED WATER OUTLET TEMP., DEGREE C
C     OUT(2)---CHILLED WATER FLOWRATE, KG/HR
C     OUT(3)---ENERGY INPUT, KJ/HR
C
      DIMENSION XIN(3),OUT(3),INFO(8)
      INFO(6)=3
      OUT(2)=XIN(2)
      IF(XIN(3).NE.1.0)  GO TO 10
      IF(XIN(1).LE.7.22)  GO TO 10
      OUT(1)=7.22
      OUT(3)=XIN(2)*4.184*(XIN(1)-7.22)
      GO TO 20
   10 OUT(1)=XIN(1)
      OUT(3)=0.0
   20 CONTINUE
      RETURN
      END
C
      SUBROUTINE TYPE31 (TIME,XIN,OUT,T,DTDT,PAR,INFO)
C
C     ENERGY RELIEF HEAT EXCHANGER FOR SOLAR ENERGY COLLECTOR
C
C     XIN(1)---INLET FLUID TEMP. DEGREE C
C     XIN(2)---MASS FLOW RATE, KG/HR
C
C     OUT(1)---OUTLET FLUID TEMP. DEGREE C
C     OUT(2)---MASS FLOW RATE, KG/HR
C     OUT(3)---ENERGY DUMPED, KJ/HR
C
C     PAR(1)---MAX. OUTLET FLUID TEMP. DEGREE C
C              SET TO THE MAX. HOT WATER STORAGE TANK TEMP.
C     PAR(2)---SPECIFIC HEAT OF COLLECTOR FLUID, KJ/KG-C
C
      DIMENSION XIN(2),OUT(3),PAR(2),INFO(8)
      INFO(6)=3
      IF(XIN(2).LE.0.0)  GO TO 10
      IF(XIN(1).LE.PAR(1))  GO TO 10
      OUT(1)=PAR(1)
      OUT(2)=XIN(2)
      OUT(3)=XIN(2)*PAR(2)*(XIN(1)-OUT(1))
      GO TO 20
   10 OUT(1)=XIN(1)
      OUT(2)=XIN(2)
      OUT(3)=0.0
   20 RETURN
      END
```

```
      SUBROUTINE TYPE32 (TIME,XIN,OUT,T,DTDT,PAR,INFO)
C
C     HEAT EXECHANGER
C
C
C     XIN(1)--TEMP. OF THE INLET HOT SIDE FLUID, DEGREE C
C     XIN(2)--MASS FLOW RATE OF THE HOT SIDE FLUID, KG/HR
C     XIN(3)--TEMP. OF THE INLET COLD SIDE FLUID, DEGREE C
C     XIN(4)--MASS FLOW RATE OF THE COLD SIDE FLUID, KG/HR
C
C     OUT(1)--TEMP. OF THE OUTLET HOT SIDE FLUID, DEGREE C
C     OUT(2)--MASS FLOW RATE OF THE HOT SIDE FLUID, KG/HR
C     OUT(3)--TEMP. OF THE OUTLET COLD SIDE FLUID, DEGREE C
C     OUT(4)--MASS FLOW RATE OF THE COLD SIDE FLUID, KG/HR
C
C     PAR(1)--EFFECTIVENESS OF HEAT EXCHANGER
C     PAR(2)--SPECIFIC HEAT OF THE HOT SIDE FLUID, KJ/KG-C
C     PAR(3)--SPECIFIC HEAT OF THE COLD  SIDE FLUID, KJ/KG-C
C
      DIMENSION XIN(4),OUT(4),PAR(3),INFO(8)
      INFO(6)=4
      IF(XIN(2).EQ.0.0)  GO TO 20
      Q=PAR(1)*(XIN(1)-XIN(3))
      OUT(1)=XIN(1)-Q
      OUT(3)=XIN(3)+Q*XIN(2)*PAR(2)/XIN(4)/PAR(3)
      OUT(2)=XIN(2)
      OUT(4)=XIN(4)
      GO TO 50
   20 OUT(1)=XIN(1)
      OUT(2)=XIN(2)
      OUT(3)=XIN(3)
      OUT(4)=XIN(4)
   50 RETURN
      END
C
C
      SUBROUTINE TYPE33 (TIME,XIN,OUT,T,DTDT,PAR,INFO)
C
C     .AND.---.OR. CONTROLLER
C
C
C     XIN(1)--FIRST INPUT CONTROL SIGNAL
C     XIN(2)--SECOND INPUT CONTROL SIGNAL
C
C     OUT(1)--OUTPUT CONTROL SIGNAL
C
C     PAR(1)--MODE INDICATOR
C             =1, INDICATE .AND.
C             =2, INDICATE .OR.
C
C
      DIMENSION XIN(2), OUT(1), PAR(1), INFO(8)
      INFO(6)=1
      IF(PAR(1).EQ.2.0)  GO TO 10
```

```
      OUT(1)=XIN(1)*XIN(2)
      GO TO 20
  10  OUT(1)=XIN(1)+XIN(2)
      IF(OUT(1).EQ.2.0)  OUT(1)=1.0
  20  RETURN
      END
```

```
C
C

      SUBROUTINE TYPE34 (TIME,XIN,OUT,T,DTDT,PAR,INFO)

C
C  ROOM AIR TEMPERATURE MODEL WITH AIR HANDLING UNIT
C
C  XIN(1)---TEMP. OF THE INLET CHILLED WATER, DEGREE C
C  XIN(2)---MASS FLOWRATE OF CHILLED WATER, KG/HR
C  XIN(3)---COOLING LOAD
C  XIN(4)---AIR HANDLING UNIT CONTROL SIGNAL
C
C  OUT(1)---TEMP. OF THE OUTLET CHILLED WATER, DEGREE C
C  OUT(2)---MASS FLOWRATE OF CHILLED WATER, KG/HR
C  OUT(3)---ROOM AIR TEMPERATURE, DEGREE C
C
C  PAR(1)---ROOM TRANSFER FUNCTION COEFFICIENT, G(0),
C                    IN BTU/HR-F
C  PAR(2)---ROOM TRANSFER FUNCTION COEFFICIENT, G(1),
C                    IN BTU/HR-F
C  PAR(3)---ROOM TRANSFER FUNCTION COEFFICIENT, G(2),
C                    IN BTU/HR-F
C  PAR(4)---SUM OF THE ROOM TRANSFER FUNCTION COEFFICIENT,
C                  G(0)+G(1)+G(2),   IN BTU/HR-F
C  PAR(5)---ROOM TRANSFER FUNCTION COEFFICIENT,  P(0)
C  PAR(6)---ROOM TRANSFER FUNCTION COEFFICIENT,  P(1)
C  PAR(7)---THE CONSTANT ROOM TEMPERATURE USED WHEN
C              CALCULATING THE COOLING LOAD,  DEGREE F
C  PAR(8)---THE THROTTLING RANGE OF THE COOLING UNIT,
C                    IN DEGREE F
C  PAR(9)---MAXIMUM HEAT EXTRACTION CAPABILITY OF THE
C                  COOLING UNIT, IN BTU/HR
C  PAR(10)---MINIMUM HEAT EXTRACTION CAPABILITY OF THE
C                  COOLING UNIT, IN BTU/HR
C  PAR(11)---TIME INTERVAL USED FOR THE SIMULATION
C
C

      DIMENSION XIN(4),OUT(3),PAR(11),INFO(8),ER(12),
     1                   Q(12),TEMP(24)
      DATA   ER,Q/24*0.0/, TEMP/24*80.0/, TIME1/-1.0/
      DATA   ERO,QO,TO/2*0.0,80.0/
      INFO(6)=3
      NT=1.0/PAR(11)+0.5
      XNT=FLOAT(NT)
C
C  INITIALIZE THE HEAT EXTRACTION RATE, COOLING LOAD,
C  AND ROOM AIR TEMPERATURE
C
      IF(TIME1.EQ.TIME)  GO TO 20
```

```
      ER1=0.0
      Q1=0.0
      T2=0.0
      T1=0.0
C
C     IF THE TIME STEP IS LESS THAN ONE HOUR, COMPUTE THE
C     AVERAGE ROOM AIR TEMPERATURES OF PREVIOUS TWO HOURS AND
C     THE AVERAGE HEAT EXTRACTION RATE AND COOLING LOAD OF THE
C     PREVIOUS HOUR
C
      IF(NT.LE.1)  GO TO 6
      NT1=NT-1
      DO 5 I=1,NT1
      J=NT-I
      JJ=J+1
      K=NT+J
      KK=K+1
      ER(JJ)=ER(J)
      Q(JJ)=Q(J)
      TEMP(KK)=TEMP(K)
      ER1=ER1+ER(J)
      Q1=Q1+Q(J)
      T2=T2+TEMP(K)
    5 CONTINUE
    6 ER(1)=ERO
      ER1=(ER1+ERO)/XNT
      Q(1)=QO
      Q1=(Q1+QO)/XNT
      TEMP(NT+1)=TEMP(NT)
      T2=(T2+TEMP(NT))/XNT
      IF(NT.LE.1)  GO TO 11
      DO 10 I=1,NT1
      J=NT-I
      JJ=J+1
      TEMP(JJ)=TEMP(J)
      T1=T1+TEMP(J)
   10 CONTINUE
   11 TEMP(1)=TO
      T1=(T1+TO)/XNT
      TIME1=TIME
C
C     COMPUTE THE HEAT EXTRACTION RATE, ERO, AND THE ROOM AIR
C     TEMPERATURE, TO
C
   20 QO=XIN(3)/1.05435
      IR=PAR(7)*PAR(4)-(PAR(2)*T1+PAR(3)*T2)+
     1          (PAR(5)*QO+PAR(6)*Q1)-(PAR(6)*ER1)
      IF(XIN(4).NE.1.0)  GO TO 30
      IF(INFO(7).GE.3)   RETURN
      S=(PAR(9)-PAR(10))/PAR(8)
      WT=(PAR(9)+PAR(10))/2.0-S*PAR(7)
      ERO=WT*PAR(1)/(S+PAR(1))+IR*S/(S+PAR(1))
      IF(ERO.GT.PAR(9))   ERO=PAR(9)
      IF(ERO.LT.PAR(10))   ERO=PAR(10)
```

```
C
C     INTERPOLATE THE ROOM AIR TEMPERATURE
C
      TO=TEMP(1)+PAR(11)*((IR-ERO)/PAR(1)-TEMP(1))
      OUT(1)=XIN(1)+ERO*1.05435/4.184/XIN(2)
      GO TO 40
C
C     WHEN THE AIR HANDLING UNIT IS TURNED OFF
C
   30 ERO=0.0
      TO=TEMP(1)+PAR(11)*(IR/PAR(1)-TEMP(1))
      OUT(1)=XIN(1)
   40 OUT(3)=(TO-32.0)*5.0/9.0
      OUT(2)=XIN(2)
      RETURN
      END
C
C

      SUBROUTINE TYPE35 (TIME,XIN,OUT,T,DTDT,PAR,INFO)
C
C     SOLAIRE 25 TON ABSORPTION CHILLER.
C     COOLING TOWER IS INCORPERATED IN THIS PROGRAM
C
C
C
C     XIN(1)---TEMP. OF INLET HOT WATER IN DEGREE C
C     XIN(2)---MASS FLOW RATE OF HOT WATER IN KG/HR
C                     (=19679 KG/HR)
C     XIN(3)---TEMP. OF INLET CHILLED WATER IN DEGREE C
C     XIN(4)---MASS FLOW RATE OF CHILLED WATER IN KG/HR
C                     (=13621 KG/HR)
C     XIN(5)---OUT DOOR WET BULB TEMP. IN DEGREE C
C     XIN(6)---CONTROL SIGNAL, =1 CHILLER IS TURNED ON, =0 OFF
C
C     OUT(1)---TEMP. OF OUTLET HOT WATER IN DEGREE C
C     OUT(2)---MASS FLOW RATE OF HOT WATER IN KG/HR
C                     (=19679 KG/HR)
C     OUT(3)---TEMP. OF OUTLET CHILLED WATER IN DEGREE C
C     OUT(4)---MASS FLOW RATE OF CHILLED WATER IN KG/HR
C                     (=13621 KG/HR)
C     OUT(5)---ENERGY INPUT TO THE CHILLER IN KJ/HR
C     OUT(6)---COOLING PRODUCED BY THE CHILLER IN KJ/HR
C     OUT(7)---COP OF THE ABSORPTION CHILLER
C
C
C     PAR(1)---DESIRED MINIMUN CHILLED WATER OUTLET TEMPERATURE,
C                     DEGREE C
C
C
      DIMENSION XIN(6),OUT(7),INFO(8),PAR(1)
      INFO(6)=7
      DATA IFLAG/1/, TCDO/30.0/
C
C     INITIALIZE THE FLAGS
C        TLOFF---TIME WHEN THE CHILLER WAS LAST TURNED OFF
```

```
C           TLON--TIME WHEN THE CHILLER WAS LAST TURNED ON
C
      IF(IFLAG.NE.1)  GO TO 10
      TLOFF=TIME-0.25
      TLON=TIME-0.5
      IFLAG=0
   10 CONTINUE
C
      IF(XIN(6).NE.1.0)  GO TO 90
C
C   COOLING TOWER
C
      TCDI=83.4854-5.59771*XIN(5)+0.115708*XIN(5)*XIN(5)
     1      -2.03676*TCDO+0.00825167*TCDO*TCDO+0.188583*XIN(5)
     2        *TCDO-0.0036081*XIN(5)*XIN(5)*TCDO-0.000857333
     3           *XIN(5)*TCDO*TCDO+0.0000180777*XIN(5)
     4              *XIN(5)*TCDO*TCDO
      IF(TCDI.LT.24.0)  TCDI=24.0
C
C
C   ABSORPTION CHILLER
C
C
C   MAXIMUM TEMPERATURE
C
      TMAX=-51.991+0.70636*XIN(1)+1.8395*TCDI-0.144089*PAR(1)
     1          -0.36014E-2*XIN(1)*XIN(1)-0.42221E-1*TCDI*TCDI
     2          -0.14912E-1*PAR(1)*PAR(1)+0.112911E-2*XIN(1)
     3            *TCDI+0.618492E-2*XIN(1)*PAR(1)
     4              +0.35438E-1*TCDI*PAR(1)
C
C   ACTUAL CAPACITY
C
      IF(XIN(3).LE.TMAX)  GO TO 20
      OUT(3)=XIN(3)-TMAX+PAR(1)
      GO TO 25
   20 OUT(3)=PAR(1)
   25 OUT(4)=13620.0
      DELT=XIN(3)-OUT(3)
      CHKOFF=TIME-TLOFF
      IF(CHKOFF.LE.0.25)  GO TO 30
      OUT(6)=OUT(4)*4.184*(XIN(3)-OUT(3))
      GO TO 35
C
C   COOLING PRODUCED IS ZERO AT START-UP PERIOD
C
   30 OUT(6)=0.0
      OUT(3)=XIN(3)
   35 CONTINUE
C
C   ENERGY INPUT
C
      OUT(5)=-0.524245E6-0.769823E5*XIN(1)+0.213556E6*TCDI
     1          +0.325587E6*DELT+0.116977E4*XIN(1)*XIN(1)
```

```
      2                -0.836132E3*TCDI*TCDI+0.127964E5*DELT*DELT
      3                  -0.257489E4*XIN(1)*TCDI-0.788791E4*XIN(1)
      4                   *DELT+0.879459E4*TCDI*DELT
        OUT(2)=19680.0
        OUT(1)=XIN(1)-OUT(5)/OUT(2)/4.184
C
        OUT(7)=OUT(6)/OUT(5)
        TCDO=TCDI+(OUT(5)+OUT(6))/85214.2
        TLON=TIME
        GO TO 100
C
C    WHEN THE CHILLER IS TURNED OFF
C
  90    CHKON=TIME-TLON
        IF(CHKON.LT.0.25)   GO TO 95
        TLOFF=TIME
  95    OUT(1)=XIN(1)
        OUT(2)=XIN(2)
        OUT(3)=XIN(3)
        OUT(4)=XIN(4)
        OUT(5)=0.0
        OUT(6)=0.0
        OUT(7)=-1.0
  100   CONTINUE
        RETURN
```

```
***
***    SAMPLE INPUT
***

SIMULATION 0.0,   4416.0,   0.125

 UNIT 1   TYPE 9    DATA READER
    PARAMETERS 4
     4,   1.0,   9.0,   1.0
(2F4.1,2F8.1)

 UNIT 2   TYPE 1    SOLAR ENERGY COLLECTOR
    PARAMETERS 7
     1.0,   350.0,   0.95,   3.515,   0.94,   15.0,   0.8
    INPUTS 4
     5,1     5,2    1,1     1,3
     70.0,   0.0,   20.0,   0.0

 UNIT 3   TYPE 32   COLLECTOR TO HOT WATER TANK HEAT EXCHANGER
    PARAMETERS 3
     0.75,   3.515,   4.184
    INPUTS 4
     6,1     6,2    10,1   10,2
     50.0,   0.0,   50.0,   20000.0

 UNIT 4   TYPE 11   TIE PIECE AT THT COLLECTOR INLET
    PARAMETERS 1
     1.0
    INPUTS 4
     3,1     3,2    7,1     7,2
     50.0,   0.0,   50.0,   0.0

 UNIT 5   TYPE 3    COLLECTOR PUMP
    PARAMETERS 1
     10000.0
    INPUTS 3
      4,1    4,2   9,1
     50.0,   0.0,   0.0

 UNIT 6   TYPE 11   FLOW DIVERTER AT COLLECTOR OUTLET
    PARAMETERS 1
     2.0
    INPUTS 3
     2,1     2,2   8,1
     50.0,   0.0,   0.0

 UNIT 7   TYPE 31   COLLECTOR ENERGY RELIEF HEAT EXCHANGER
    PARAMETERS 2
     95.0,   3.515
    INPUTS 2
     6,3   6,4
     50.0,   0.0

 UNIT 8   TYPE 2    COLLECTOR FLOW DIVERTER CONTROLLER
```

```
PARAMETERS 3
 3,  0.0,  0.0
INPUTS 3
 10,1  0,0    8,1
 50.0,  95.0,  0.0


UNIT 9 TYPE 2  COLLECTOR PUMP CONTROLLER
  PARAMETERS 3
  3,  8.0,  4.0
  INPUTS 3
  2,1    10,1  9,1
  50.0,  50.0,  0.0


UNIT 10  TYPE 4  HOT WATER STORAGE TANK
  PARAMETERS 5
  30.0,  1.5,  4.184,  1000.0,  1.0
  INPUTS 5
  3,3      3,4       12,1  12,2  0,0
  50.0,  20000.0,  70.0,  0.0,  25.0
 DERIVATIVES 1
  70.0


UNIT 11 TYPE 4  CHILLED WATER STORAGE TANK
  PARAMETERS 5
  30.0,  1.5,  4.184,  1000.0,  1.0
  INPUTS 5
  13,1  13,2  11,3  11,4  0,0
  5.0,  0.0,  5.0,  0.0,  25.0
 DERIVATIVES 1
  5.0


UNIT 12  TYPE 35  ABSORPTION CHILLER
  PARAMETERS 1
  4.45
  INPUTS 6
  14,1  14,2  16,1  16,2  1,2    19,1
  50.0,  0.0,  5.0,  0.0,  25.0,  0.0


UNIT 13  TYPE 29  AUXILIARY CHILLER
  PARAMETERS 1
  7.22
  INPUTS 3
  12,3  12,4  20,1
  5.0,  0.0,  0.0


UNIT 14 TYPE 3  HOT WATER TO CHILLER PUMP
  PARAMETERS 1
  19680.0
  INPUTS 3
  10,3  10,4  19,1
  50.0,  0.0,  0.0


UNIT 15  TYPE 3  CHILLED WATER PUMP
  PARAMETERS 1
```

```
      13620.0
      INPUTS 3
       11,1  11,2  0,0
       5.0,  0.0,  1.0


UNIT 16 TYPE 34  ROOM AND AIR HANDLING UNIT
   PARAMETERS 11
      15190.0,  -15510.0,  583.0,  260.1,  1.0,  -0.87,
      77.0,  3.0,  306000.0,  0.0,  0.125
   INPUTS 4
      15,1  15,2     1,4  21,1
      5.0,  13620.0,  0.0,  0.0


UNIT 17  TYPE 2  HOT WATER PUMP CONTROLLER
   PARAMETERS 3
      3,  10.0,  0.0
   INPUTS 3
      10,3   0,0     17,1
      50.0,  72.0,  0.0


UNIT 18 TYPE 2  CHILLED WATER CONTROLLER
   PARAMETERS 3
      3,  2.778,  0.0
   INPUTS 3
      11,1  0,0     18,1
      5.0,  6.667,  0.0


UNIT 19  TYPE 33  ABSORPTION CHILLER CONTROLLER
   PARAMETERS 1
      1.0
   INPUTS 2
      17,1  18,1
      0.0,  0.0


UNIT 20  TYPE 2  AUXILIARY CHILLER CONTROLLER
   PARAMETERS 3
      3,  1.111,  0.0
   INPUTS 3
      11,1  0,0     20,1
      5.0,  9.445,  0.0


UNIT 21  TYPE 2  AIR HANDLING UNIT CONTROLLER
   PARAMETERS 3
      3,  2.222,  0.0
   INPUTS 3
      16,3   0,0     21,1
      25.0,  23.89,  0.0


UNIT 41  TYPE 24  INTEGRATOR
   PARAMETERS 1
      24.0
   INPUTS 6
      12,5  12,6  13,3  1,4  1,3  7,3
      0.0,  0.0,  0.0,  0.0,  0.0,  0.0
```

```
UNIT 42   TYPE 25   OUTPUT
  PARAMETERS 4
   24.0,   0.0,   4416.0,   10.0
  INPUTS 6
   41,1   41,2   41,3   41,4   41,5   41,6
   QE,   QC,   QAUX,   QLOAD,   HT,   QDUMP

END
```

APPENDIX C

SIMULATION RESULTS OF THE SOLAR COOLING SYSTEMS AT

THE SEVEN SOLMET STATIONS CHOSEN FOR THIS STUDY

DODGE CITY, KANSAS (I)

HOT WATER STORAGE VOLUME (M**3)	CHILLED WATER STORAGE VOLUME (M**3)	COLLECTOR AREA (M**2)	AVERAGE COP OF ABSORP. CHILLER	SOLAR FRACTION
10.0	10.0	400.0	0.448	0.632
10.0	15.0	440.0	0.489	0.694
10.0	20.0	320.0	0.556	0.680
10.0	25.0	280.0	0.592	0.665
10.0	30.0	360.0	0.580	0.727
10.0	40.0	240.0	0.624	0.661
15.0	10.0	280.0	0.523	0.639
15.0	15.0	400.0	0.509	0.770
15.0	20.0	240.0	0.592	0.635
15.0	25.0	320.0	0.581	0.747
15.0	30.0	440.0	0.561	0.838
15.0	40.0	360.0	0.593	0.808

DODGE CITY, KANSAS (II)

HOT WATER STORAGE VOLUME (M**3)	CHILLED WATER STORAGE VOLUME (M**3)	COLLECTOR AREA (M**2)	AVERAGE COP OF ABSORP. CHILLER	SOLAR FRACTION
20.0	10.0	360.0	0.492	0.733
20.0	15.0	240.0	0.578	0.633
20.0	20.0	400.0	0.540	0.832
20.0	25.0	440.0	0.544	0.867
20.0	30.0	320.0	0.592	0.768
20.0	40.0	280.0	0.614	0.722
25.0	10.0	440.0	0.472	0.807
25.0	15.0	360.0	0.543	0.798
25.0	20.0	280.0	0.585	0.708
25.0	25.0	400.0	0.558	0.856
25.0	30.0	240.0	0.613	0.659
25.0	40.0	320.0	0.605	0.786

DODGE CITY, KANSAS (III)

HOT WATER STORAGE VOLUME (M**3)	CHILLED WATER STORAGE VOLUME (M**3)	COLLECTOR AREA (M**2)	AVERAGE COP OF ABSORP. CHILLER	SOLAR FRACTION
30.0	10.0	320.0	0.527	0.721
30.0	15.0	280.0	0.573	0.702
30.0	20.0	360.0	0.564	0.823
30.0	25.0	240.0	0.610	0.659
30.0	30.0	400.0	0.573	0.879
30.0	40.0	440.0	0.568	0.917
40.0	10.0	240.0	0.559	0.608
40.0	15.0	320.0	0.568	0.769
40.0	20.0	440.0	0.545	0.911
40.0	25.0	360.0	0.581	0.840
40.0	30.0	280.0	0.612	0.735
40.0	40.0	400.0	0.588	0.898

FORT WORTH, TEXAS

HOT WATER STORAGE VOLUME (M**3)	CHILLED WATER STORAGE VOLUME (M**3)	COLLECTOR AREA (M**2)	AVERAGE COP OF ABSORP. CHILLER	SOLAR FRACTION
10.0	30.0	360.0	0.612	0.568
10.0	40.0	400.0	0.617	0.611
15.0	20.0	240.0	0.616	0.459
15.0	25.0	280.0	0.619	0.514
20.0	15.0	400.0	0.571	0.617
25.0	10.0	320.0	0.569	0.529
25.0	15.0	360.0	0.586	0.592
30.0	10.0	280.0	0.577	0.481
30.0	20.0	360.0	0.606	0.613
40.0	40.0	440.0	0.630	0.732

EL PASO, TEXAS

HOT WATER STORAGE VOLUME (M**3)	CHILLED WATER STORAGE VOLUME (M**3)	COLLECTOR AREA (M**2)	AVERAGE COP OF ABSORP. CHILLER	SOLAR FRACTION
10.0	40.0	280.0	0.627	0.688
15.0	30.0	280.0	0.619	0.698
20.0	30.0	320.0	0.611	0.765
20.0	40.0	360.0	0.604	0.820
30.0	10.0	440.0	0.508	0.840
40.0	15.0	320.0	0.592	0.771
40.0	20.0	360.0	0.594	0.839
40.0	30.0	400.0	0.600	0.899
40.0	40.0	440.0	0.596	0.941

ALBUQUERQUE, NEW MEXICO

HOT WATER STORAGE VOLUME (M**3)	CHILLED WATER STORAGE VOLUME (M**3)	COLLECTOR AREA (M**2)	AVERAGE COP OF ABSORP. CHILLER	SOLAR FRACTION
10.0	20.0	320.0	0.536	0.783
10.0	40.0	400.0	0.570	0.879
15.0	30.0	320.0	0.574	0.879
20.0	15.0	360.0	0.506	0.895
20.0	15.0	400.0	0.490	0.923
30.0	20.0	440.0	0.500	0.984
30.0	30.0	440.0	0.521	0.991
30.0	40.0	280.0	0.598	0.852
40.0	10.0	280.0	0.541	0.796
40.0	20.0	360.0	0.539	0.944

LAKE CHARLES, LOUISIANA

HOT WATER STORAGE VOLUME (M**3)	CHILLED WATER STORAGE VOLUME (M**3)	COLLECTOR AREA (M**2)	AVERAGE COP OF ABSORP. CHILLER	SOLAR FRACTION
10.0	15.0	280.0	0.591	0.399
15.0	25.0	320.0	0.620	0.460
15.0	30.0	360.0	0.617	0.498
20.0	10.0	380.0	0.555	0.476
25.0	15.0	380.0	0.588	0.506
25.0	20.0	400.0	0.600	0.535
30.0	10.0	320.0	0.574	0.431
30.0	25.0	400.0	0.612	0.549
40.0	20.0	360.0	0.611	0.505
40.0	40.0	440.0	0.629	0.606

NASHVILLE, TENNESSEE

HOT WATER STORAGE VOLUME (M**3)	CHILLED WATER STORAGE VOLUME (M**3)	COLLECTOR AREA (M**2)	AVERAGE COP OF ABSORP. CHILLER	SOLAR FRACTION
10.0	25.0	280.0	0.610	0.480
15.0	30.0	360.0	0.614	0.576
15.0	40.0	380.0	0.615	0.604
20.0	10.0	360.0	0.541	0.531
20.0	20.0	400.0	0.584	0.609
25.0	20.0	440.0	0.579	0.656
25.0	30.0	320.0	0.624	0.550
30.0	10.0	320.0	0.565	0.506
30.0	40.0	400.0	0.621	0.647
40.0	25.0	380.0	0.614	0.626

COLUMBIA, MISSOURI

HOT WATER STORAGE VOLUME (M**3)	CHILLED WATER STORAGE VOLUME (M**3)	COLLECTOR AREA (M**2)	AVERAGE COP OF ABSORP. CHILLER	SOLAR FRACTION
10.0	15.0	340.0	0.523	0.571
10.0	30.0	420.0	0.567	0.648
15.0	20.0	400.0	0.541	0.679
15.0	40.0	300.0	0.610	0.627
20.0	10.0	360.0	0.495	0.619
20.0	25.0	280.0	0.591	0.599
25.0	40.0	360.0	0.598	0.709
30.0	10.0	420.0	0.485	0.685
30.0	25.0	340.0	0.578	0.679
40.0	30.0	400.0	0.578	0.760

VITA ^{2}

Ping-Shian Shih

Candidate for the Degree of

Doctor of Philosophy

Thesis: DESIGN PARAMETERS FOR SOLAR POWERED ABSORPTION COOLING SYSTEMS
WITH CHILLED WATER STORAGE

Major Field: Mechanical Engineering

Biographical:

Personal Data: Born in Chang-Hwa, Taiwan, June 2, 1948, the son
of Ting Liao and Show Ching Shih.

Education: Graduated from Chang-Hwa High School, Chang-Hwa, in
June, 1966; received the Bachelor of Science in Engineering
degree from National Taiwan University, Taipei, Taiwan, in
June, 1971; received the Master of Science in Mechanical
Engineering degree from the University of New Hampshire,
Durham, New Hampshire, in May, 1976; completed requirements
for the Doctor of Philosophy degree at Oklahoma State Univer-
sity in December, 1979.

Professional Experience: Second Lieutenant, Logistic Control Offi-
cer, Chinese Air Force, July, 1971, to June, 1972; teaching
assistant, Department of Mechanical Engineering, National
Taiwan University, August, 1972, to July, 1973; graduate
teaching assistant, Department of Mechanical Engineering,
University of New Hampshire, September, 1974, to June, 1975;
graduate teaching and research associate, School of Mechani-
cal and Aerospace Engineering, Oklahoma State University,
September, 1975, to October, 1979.

Professional Organizations: Student Member, American Society of
Mechanical Engineers (ASME); American Institute of Aeronau-
tics and Astronautics (AIAA); American Society of Heating,
Refrigeration and Air-Conditioning Engineers (ASHRAE).